Sulfur-Tolerant Anodes for SOFCs

Project Manager: Lane Wilson, NETL/DoE

Presenter: M. Liu

Co-Authors: Z. Cheng, Y. Choi, J. Wang, S. Zha

Center for Innovative Fuel Cell and Battery Technologies

School of Materials Science and Engineering

Georgia Institute of Technology

September 13, 2006

Philadelphia, PA

Outline

- **Technical Issues Addressed**
- **Objectives & Approach**
- **Recent Progress**
  - **The H_2S Poisoning Effect**
  - **The Proposed S-Poisoning Mechanism**
  - ***In Situ* Identification of NiS_x**
  - **Strategy for Improving S Tolerance of Ni Cermet**
    - **Modification of Ni**
    - **Effect of Electrolyte in Ni-Based Anodes**
- **Activities for the next 6-12 Months**

Technical Issues

- SOFCs have the potential for direct utilization of HC fuels or gasified coal, which often contain sulfur
- Trace amount of sulfur causes significant degradation in performance
- Desulfurization (<1 ppm) adds additional complexity & cost to SOFC system

Challenge: How to minimize the impact of small a mount of H_2S on fuel cell performance?

Objective

- To characterize the behavior of Ni-based anodes exposed to a sulfur-contaminated fuel
- To unravel the mechanism of sulfur poisoning using computational and experimental techniques
- To develop strategy for achieving sulfur tolerance and for rational design of new anode materials/structures
- To determine the practical operation window (T, V/I, H_2S) that minimizes the impact of sulfur contaminants on fuel cell performance, and
- To generate knowledge useful to the SECA industrial teams in addressing issues relevant to sulfur poisoning

Technical Approaches

Phenomenological Characterization of Sulfur Poisoning

- **Impedance spectroscopy (IS)**
- **Cell performance and anode over-potential**

Understanding Sulfur Poisoning Mechanism

- **Computational: First Principle and MD calculations**
- **Thermodynamic/kinetic analysis**
- ***In situ* Raman spectroscopy**
  - Directly identify surface species in an environment close to that in real SOFC anode chamber
  - Can be coupled with electrochemical measurement to correlate the changes in surface chemistry/structure with electrochemical response of the anode to H_2S

Development of New Strategies for sulfur tolerance

- **Modification/decoration of Ni-YSZ Surface**
- **New materials/structure**

Recent Progress

- **The H_2S Poisoning Effect**
- **The Proposed S-Poisoning Mechanism**
- **In Situ Raman Spectroscopy**
- **Strategy for Improving S Tolerance**
  - Modification of Ni
  - Effect of Electrolyte in Ni-Based Anodes

Typical Poisoning & Regeneration Processes

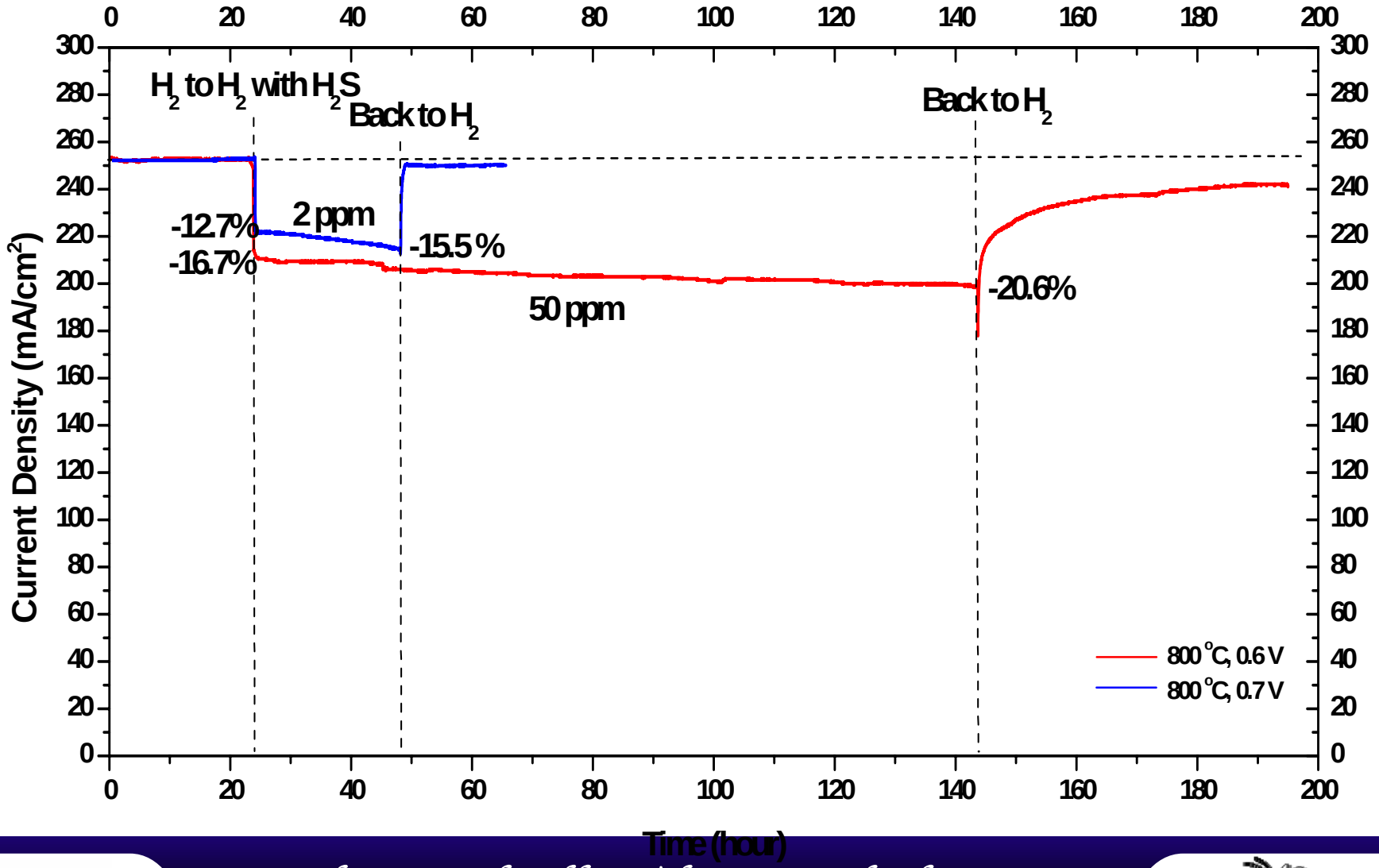

Influence of $[H_2S]$ and T

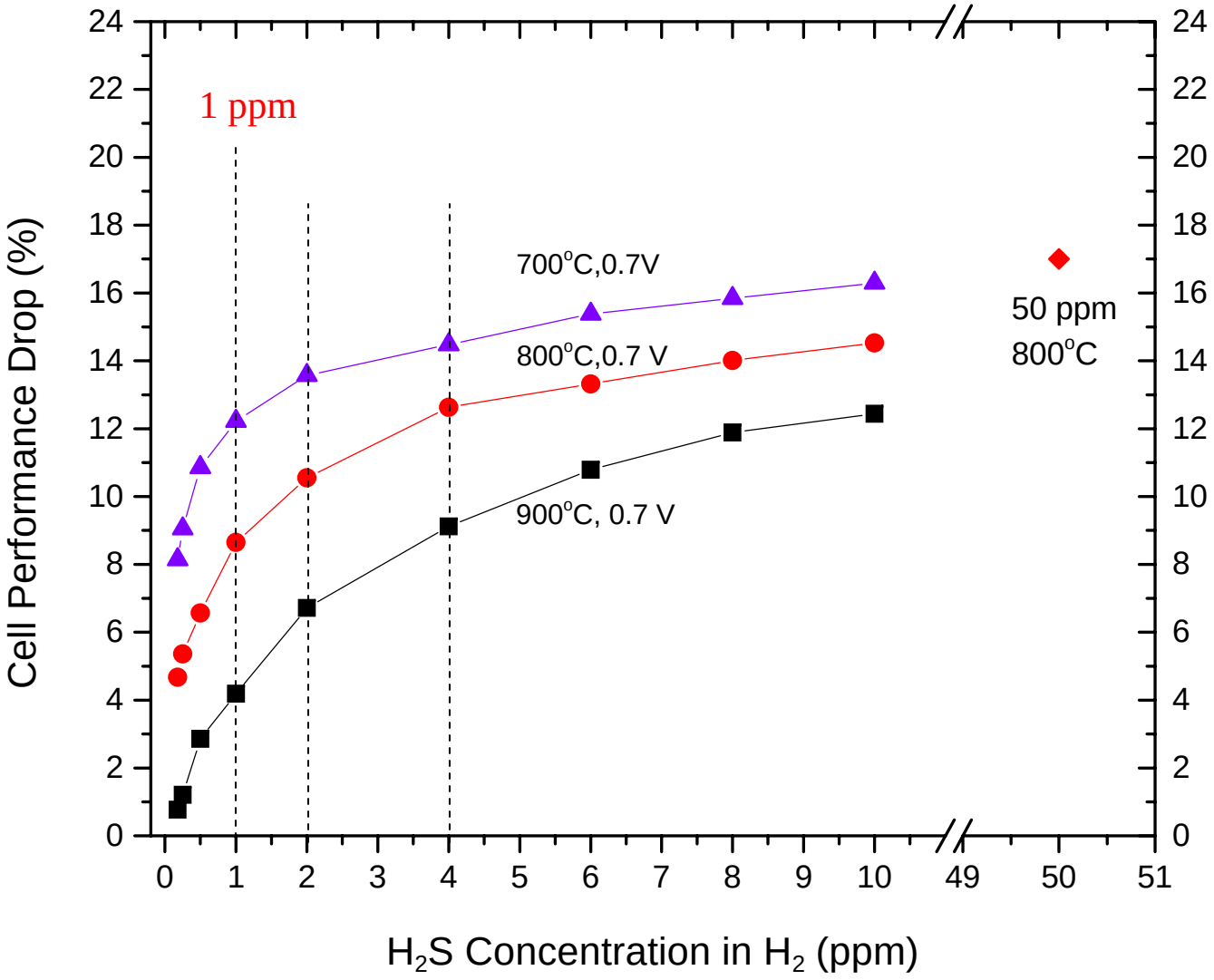

Implication - S Poisoning is a 2-Step Process

The 1st Step: Fast adsorption of sulfur occurs in minutes upon exposure to H_2S, which blocks reaction sites and leads to rapid performance degradation (reversible)

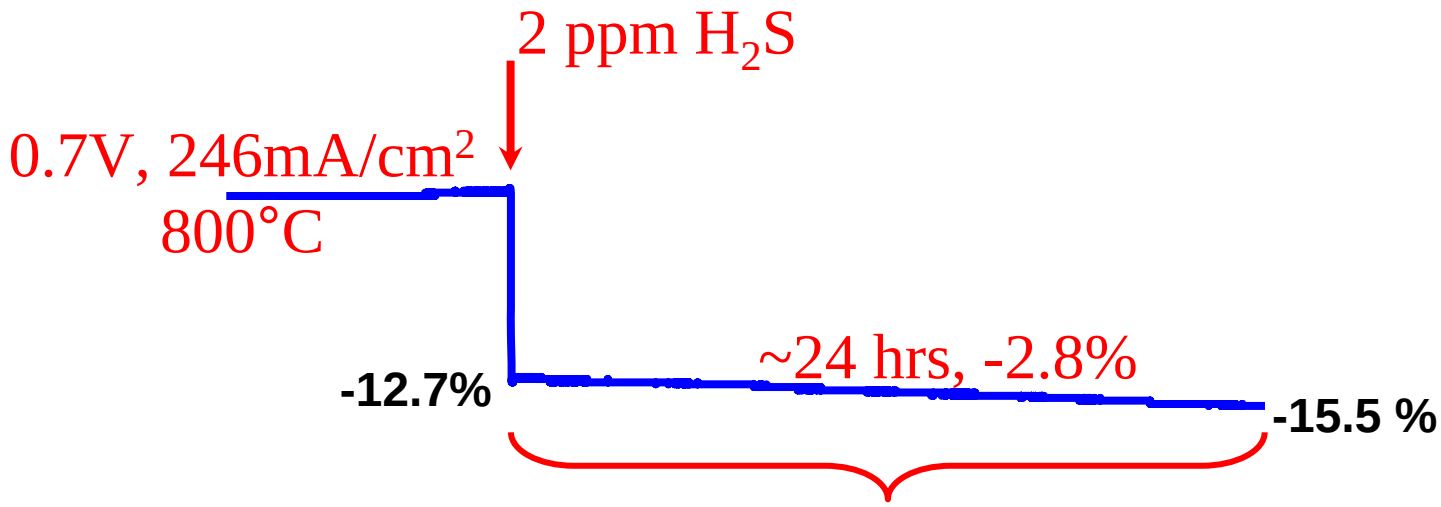

The 2nd Step: slow but continuous degradation persists in days

- **Formation of multilayer nickel sulfides on Ni surface**
- **Surface reconstruction due to adsorbed sulfur**
- **Diffusion of sulfur into Ni grains**
- **Interaction of sulfur with the electrolyte**

Rapid Sulfur Adsorption

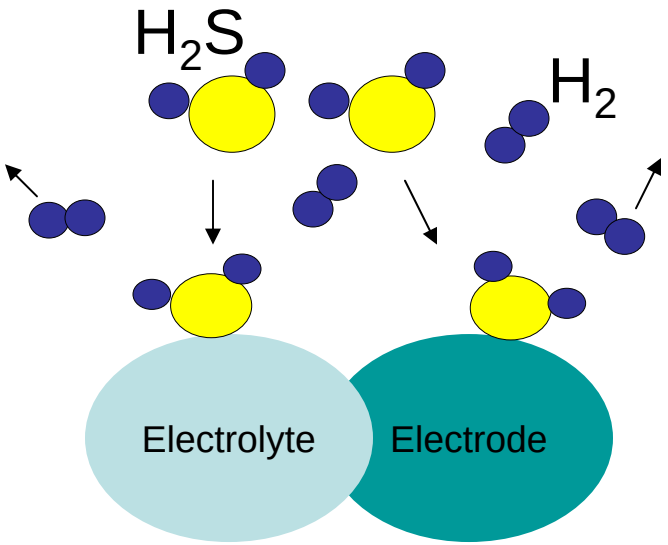

S(a) formation

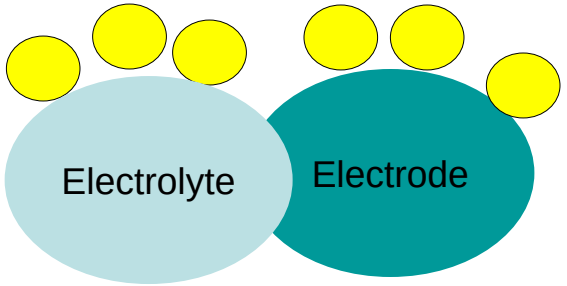

Surfaces saturated with S(a), which blocks the active sites for fuel oxidation

Influence of Cell Voltage (or Current)

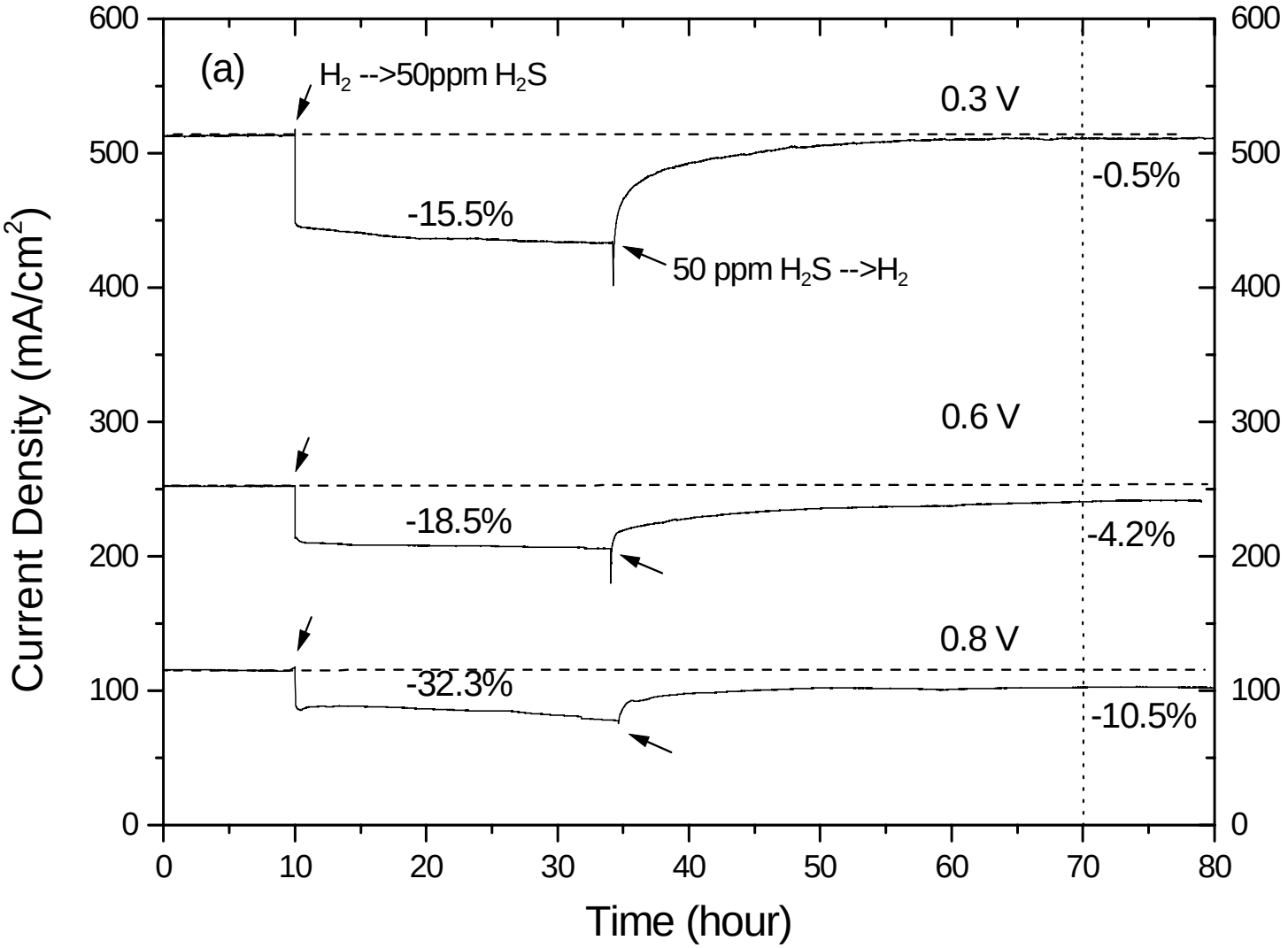

Influence of Cell Voltage (or Current)

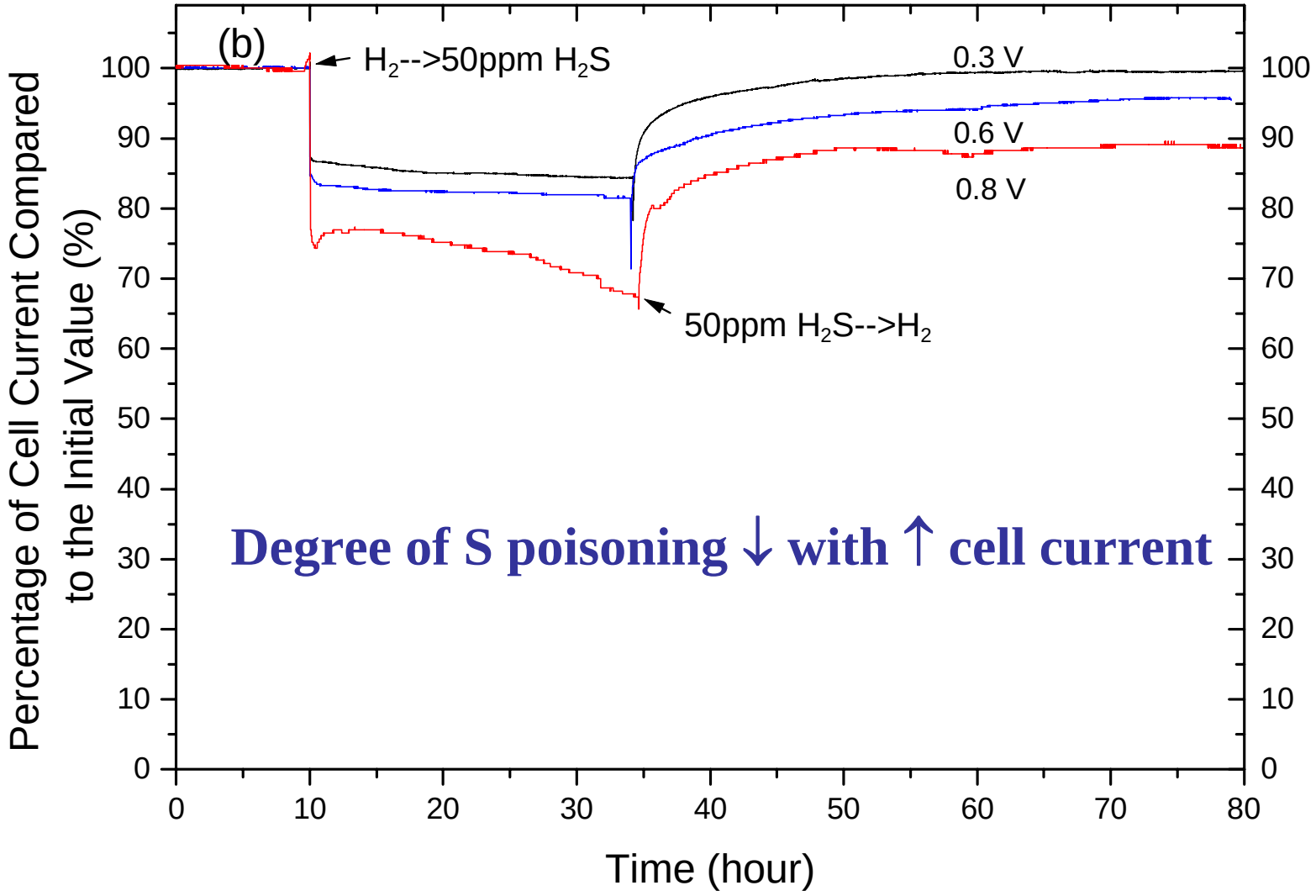

Cell Impedance Spectra at **OCV**

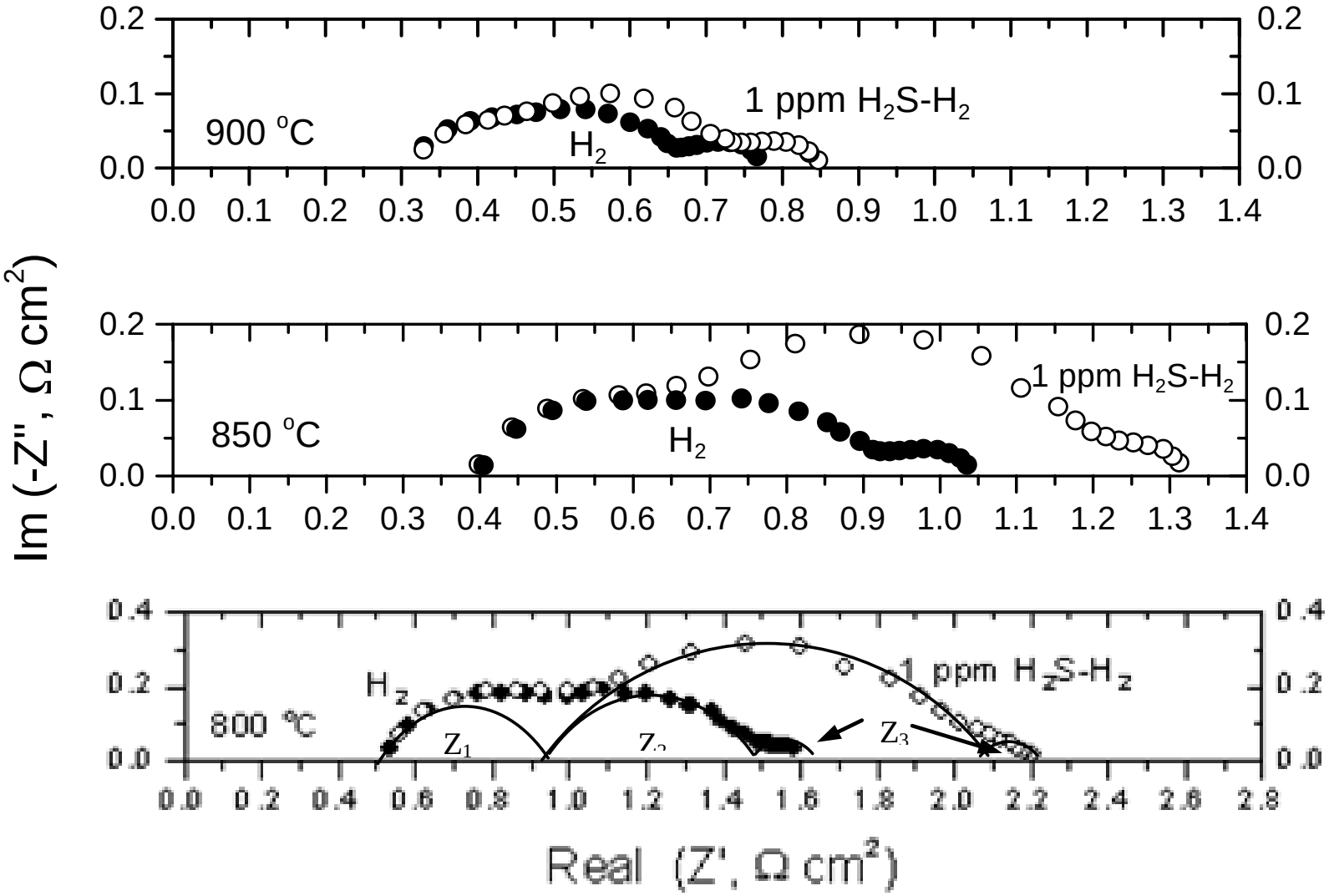

Effect of H_2S on Anodic ASR at **OCV**

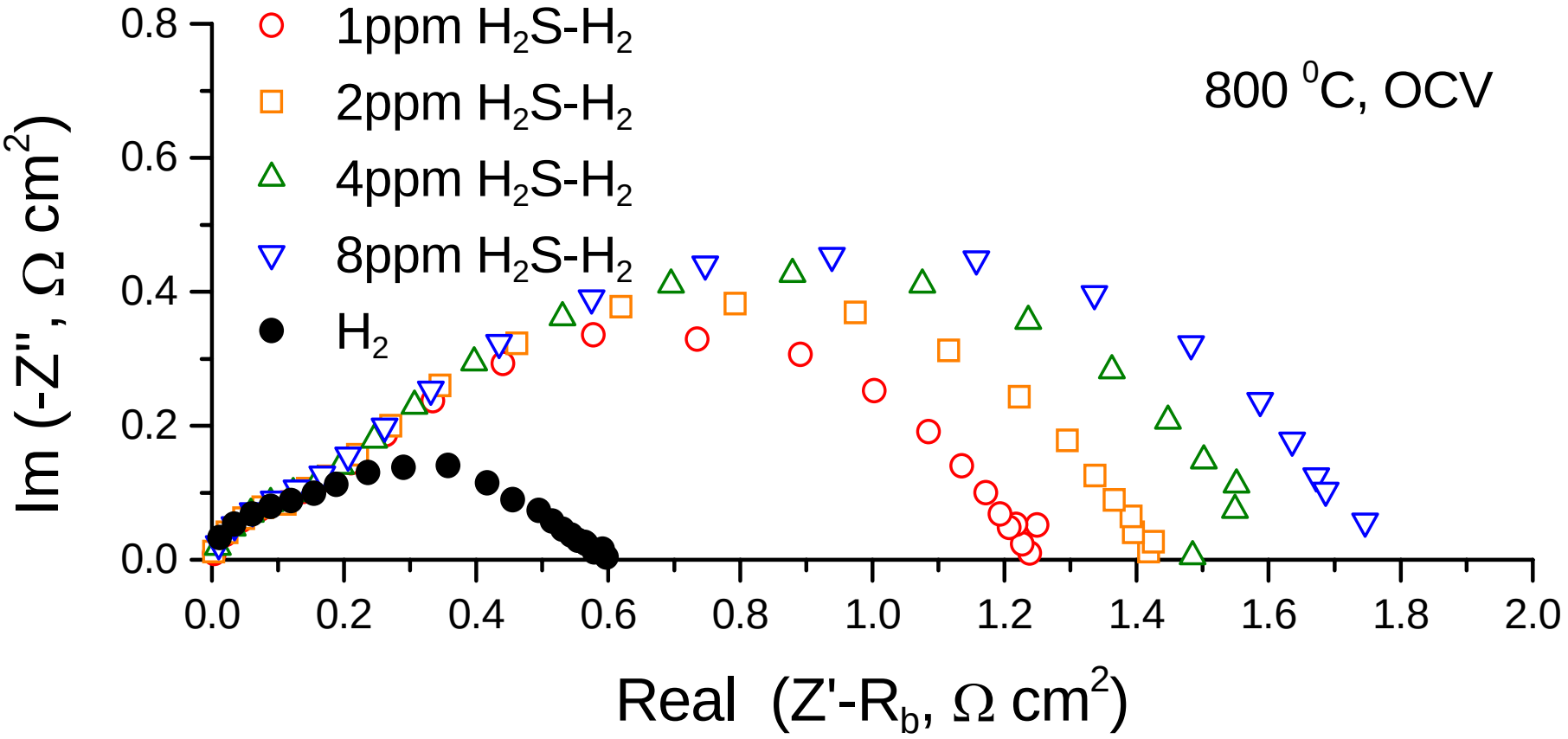

Poisoning effect is much more severe at OCV than under FC operation!

Effect of V/I on Anodic ASR

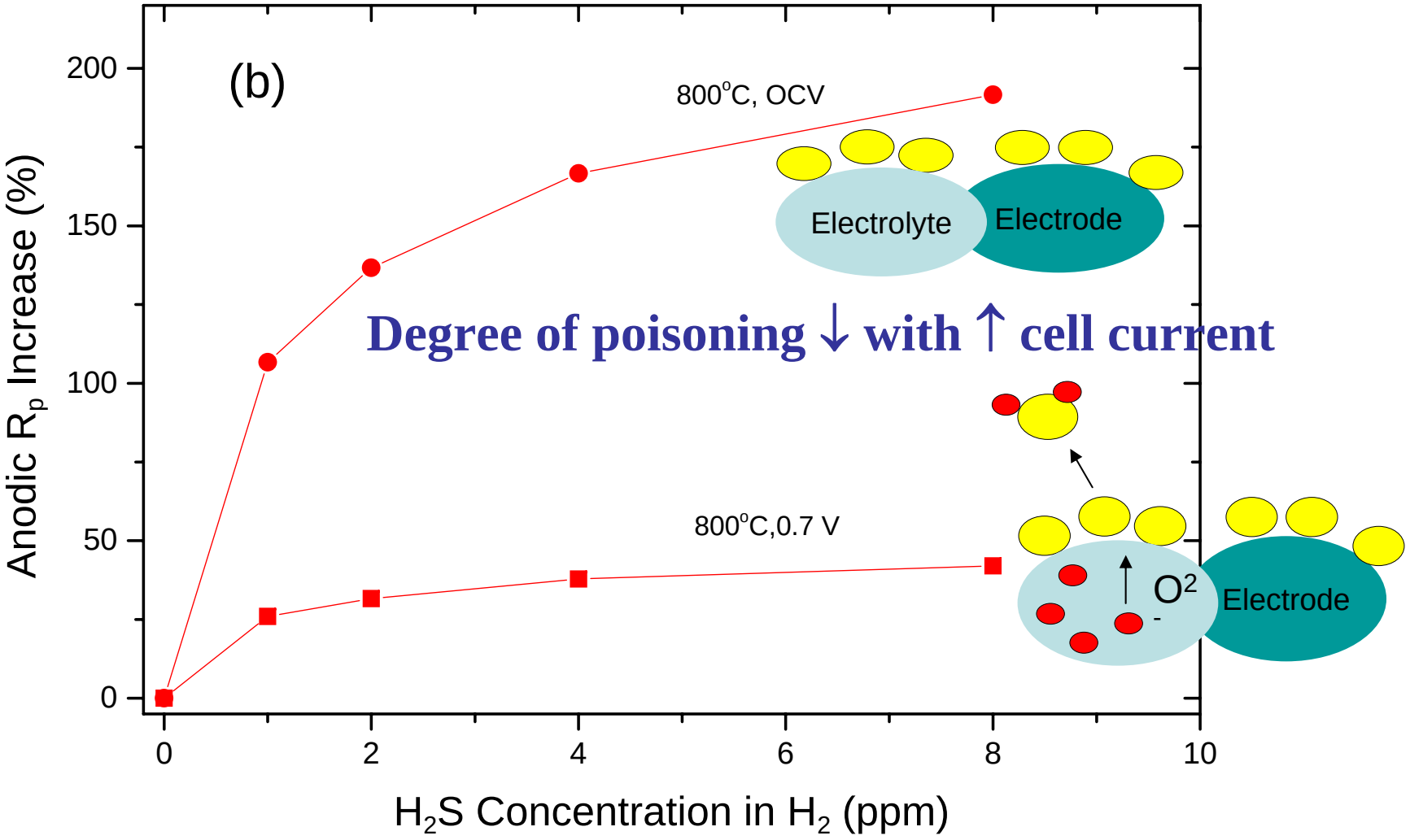

Proposed Mechanism: S→SO_2 at TPB

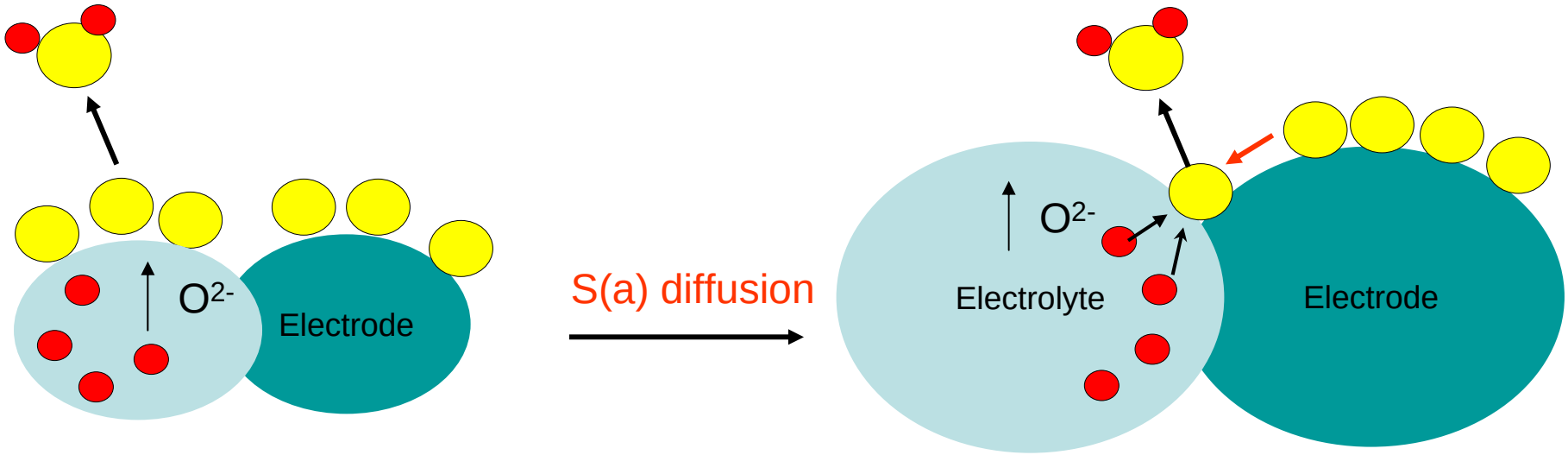

S(a) on electrolyte grain may be consumed by reacting with O^{2-} to form SO_2

Concentrated S(a) on electrode surface may diffuse to TPB to be oxidized to SO_2

Ceria or ScSZ appears to be better than YSZ in S tolerance.

Recent Progress

- The H_2S Poisoning Effect
- **The Proposed S-Poisoning Mechanism**
- In Situ Raman Spectroscopy
- Strategy for Improving S Tolerance of Ni Cermet
  - Modification of Ni
  - Effect of Electrolyte in Ni-Based Anodes

Computational method

Periodic density functional theory (DFT) calculations with VASP (Vienna Ab initio Simulation Package)

- **DFT: LDA with PW91 (GGA) correction**
- **Core pseudopotential and Cut-off energies of 300 - 600 eV**
- **Vacuum space of ~10.0 Å**

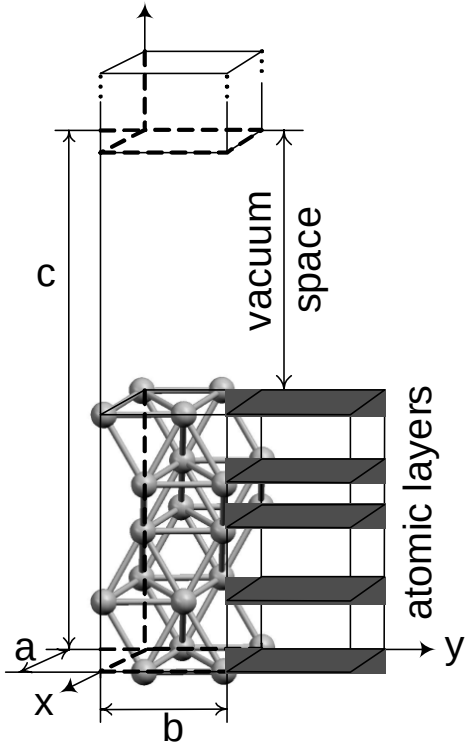

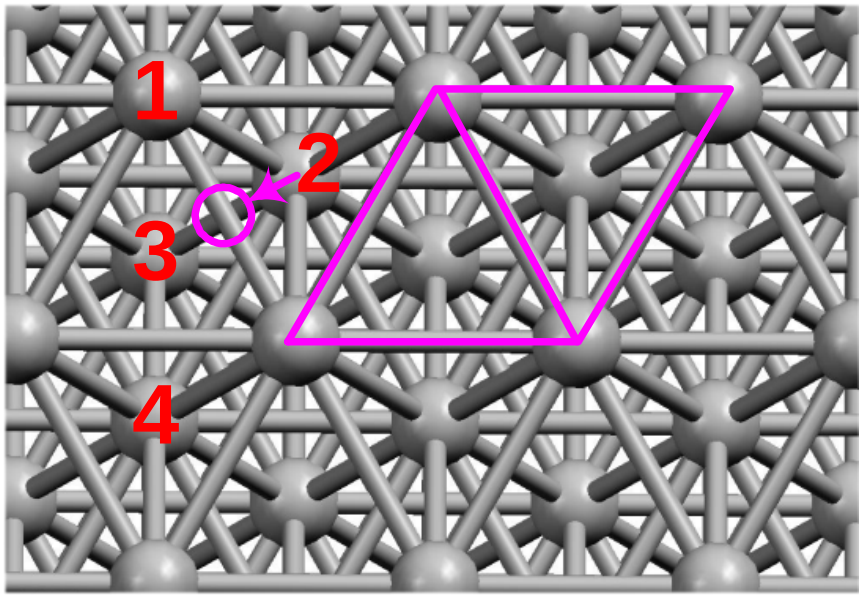

- **1, 2, 3, and 4 : atop, bridge, hcp, and fcc sites on (111) surface**

DFT Prediction of H_2S-Ni (100) Interactions

Potential energy surface (PES) in eV of $H_2S(a)$ → S(a) + 2H(a) on Ni(100)

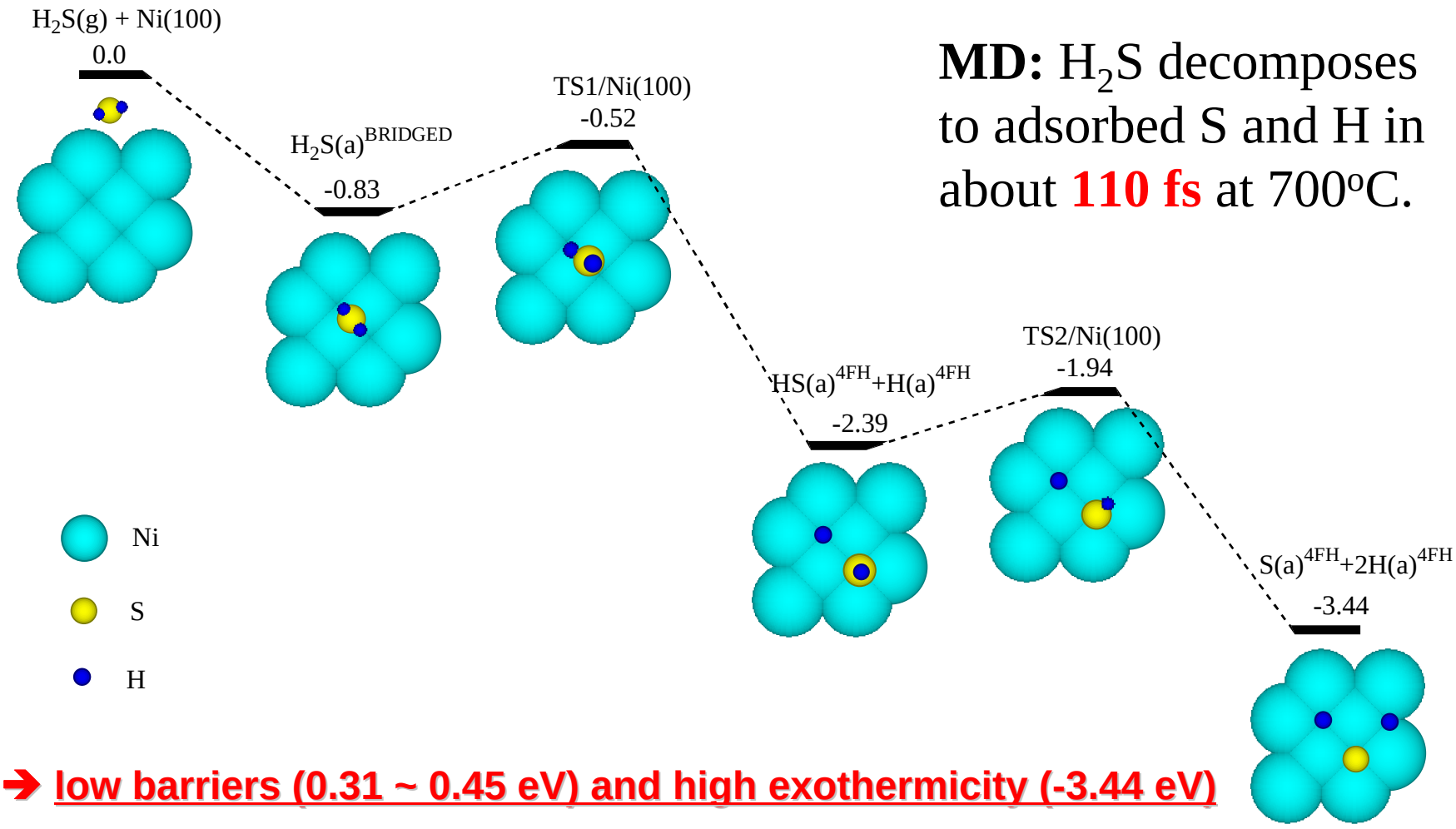

MD: H_2S decomposes to adsorbed S and H in about **110 fs** at 700°C.

➔ **low barriers (0.31 ~ 0.45 eV) and high exothermicity (-3.44 eV)**

DFT Prediction of Adsorption Energies at 0°K/Vcc

Surface models

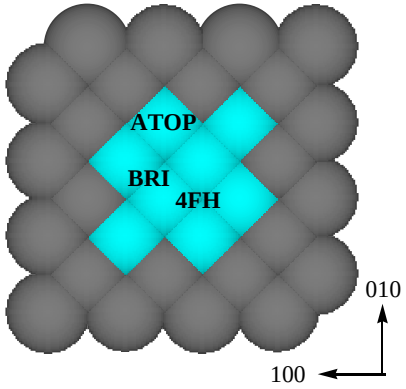

Ni(100)

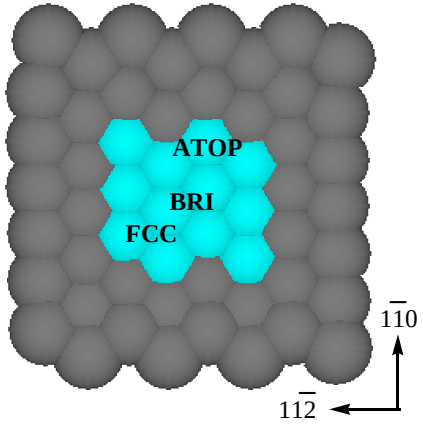

Ni(111)

Adsorption energies (eV) and bond distances (Å) of H_2S and it fragments (eV)

Ni(100)			Ni(111)		
	E_{ads}	Ni-A[a]		E_{ads}	Ni-A[a]
$H_2S(a)^{ATOP}$	-0.71	2.16	$H_2S(a)^{ATOP}$	-0.67	2.17
$H_2S(a)^{BRI}$	-0.83	2.20	$H_2S(a)^{BRI}$	-0.65	2.21
$H_2S(a)^{4FH}$	-0.62	2.30	$H_2S(a)^{FCC}$	-0.64	2.35
$HS(a)^{ATOP}$	-2.46	2.10	$HS(a)^{ATOP}$	-2.38	2.11
$HS(a)^{BRI}$	-3.18	2.17	$HS(a)^{BRI}$	-2.95	2.18
$HS(a)^{4FH}$	-3.72	2.17	$HS(a)^{FCC}$	-2.71	2.14
$S(a)^{ATOP}$	-3.71	2.00	$S(a)^{ATOP}$	-3.62	2.00
$S(a)^{BRI}$	-4.73	2.07	$S(a)^{BRI}$	-5.02	2.08
$S(a)^{4FH}$	-5.96	2.18	$S(a)^{FCC}$	-5.14	2.12
$H(a)^{ATOP}$	-2.27	1.47	$H(a)^{ATOP}$	-2.28	1.47
$H(a)^{BRI}$	-2.73	1.61	$H(a)^{BRI}$	-2.74	1.63
$H(a)^{4FH}$	-2.84	1.83	$H(a)^{FCC}$	-2.91	1.70

Effect of T and P on Predictions

- **T and p effect : DFT + thermodynamic correction**

surface1 + gas1(g) → surface2 + gas2(g)

$\Delta E = (E_{surface2} + E_{gas2}) - (E_{surface1} - E_{gas1})$ adsorption energy, T = p= 0, (DFT)

Environment effects, T, p

$\Delta G = (G_{surface2} + G_{gas2}) - (G_{surface1} - G_{gas1})$

$G(T,p)_{surface} \sim G(0,0)_{surface} = E_{surface}$

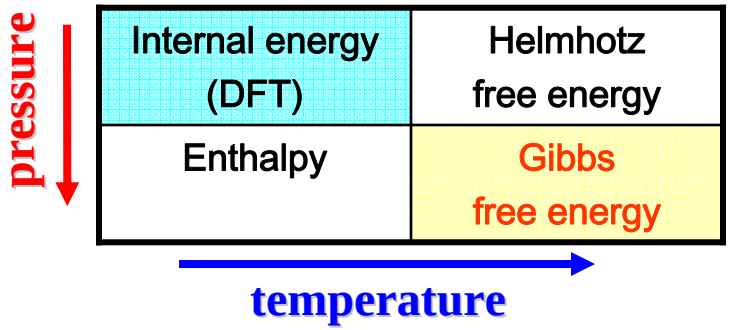

$G(T,p)_{gas} = G(0,0)_{gas} + \Delta G(0 \rightarrow T, p^0)_{gas} + \Delta G(T, p^0 \rightarrow p)_{gas}$

$= E_{gas} + H(T)_{gas} + RT*\ln(p_{gas}/p^0)$

- **Gibbs Free energy**

$\Delta G(T,p) = [(G_{surface2} - G_{surface1}) + (G_{gas2} - G_{gas1})]$

$= [\Delta E + \Delta H(T) + RT*\ln(p_{gas2}/p_{gas1})]$

* K. Reuter, M. Scheffler: Phys. Rev. B 65 (2001) 35406

Phase diagram of Ni-S system and sulfur poisoning

Boundaries

- **blue lines: the boundary of S(a)^{4FH} on Ni(100).**
- **red lines: the boundary of S(a)^{FCC} on Ni(111).**

Phases

- **upper white area: the phase of clean Ni surface.**
- **middle green area: the phase of S(a) on Ni surfaces.**
- **lower yellow area: the phase of bulk nickel sulfide, Ni_3S_2.**

Experimental observations

- **black line: the boundary between Ni and Ni_3S_2 bulk.[1]**
- **black symbols: the boundaries of the sulfur adsorption phase[2] with different "area coverage".**
- **red circles: sulfur tolerance from impedance analysis[3]**

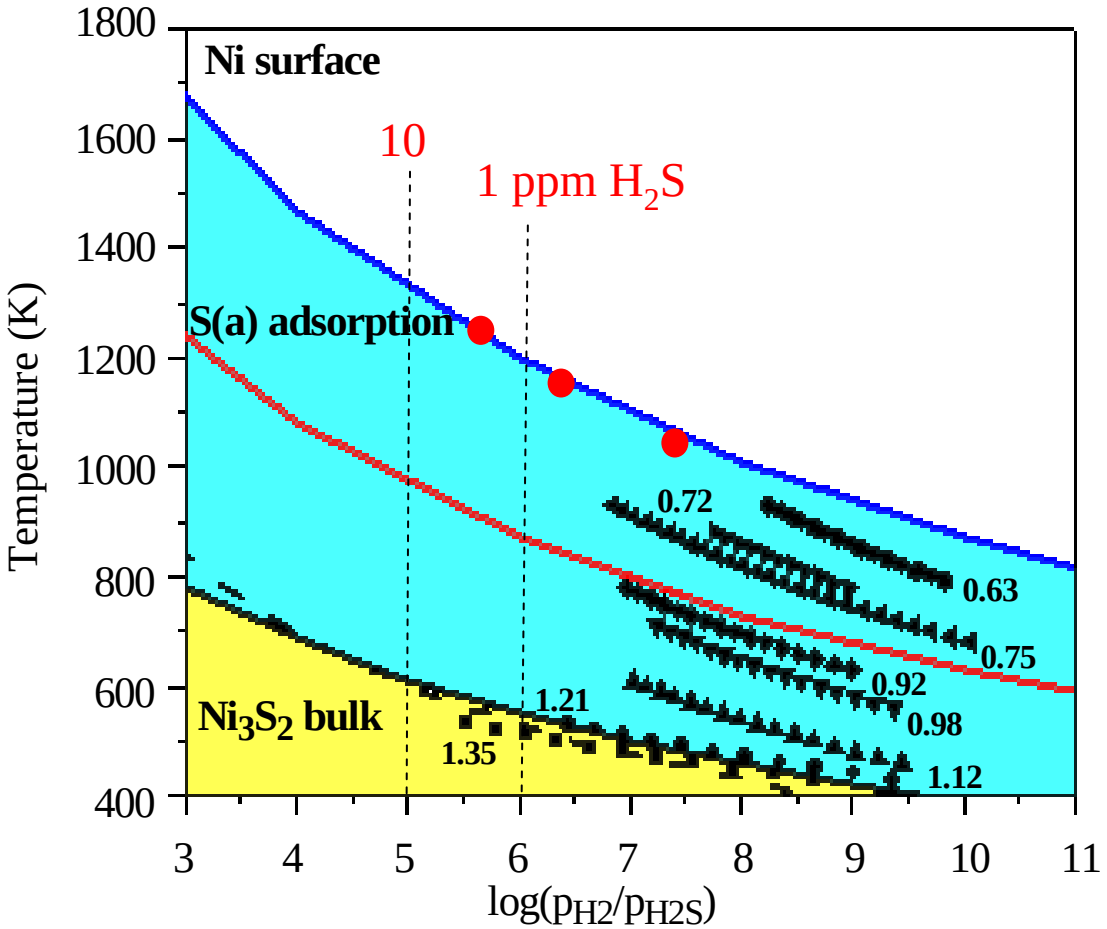

[1] Rosenqvist, T. *J. Iron Steel Inst.* **1954**, *176*, 37 (bulk phase)
[2] McCarty, J. G.; Wise, H. J. Chem. Phys. 1980, 72, 6332 (Adsorption phase)
[2] Matsuzaki, Y.; Yasuda, I. *Solid State Ionics* **2000**, *132*, 261 (S-poisoning)

Recent Progress

- The H_2S Poisoning Effect
- The Proposed S-Poisoning Mechanism
- ***In Situ* Raman Spectroscopy – 2nd Step**
- Strategy for Improving S Tolerance of Ni Cermet
  - Modification of Ni
  - Effect of Electrolyte in Ni-Based Anodes

In situ Identification of NiS_x

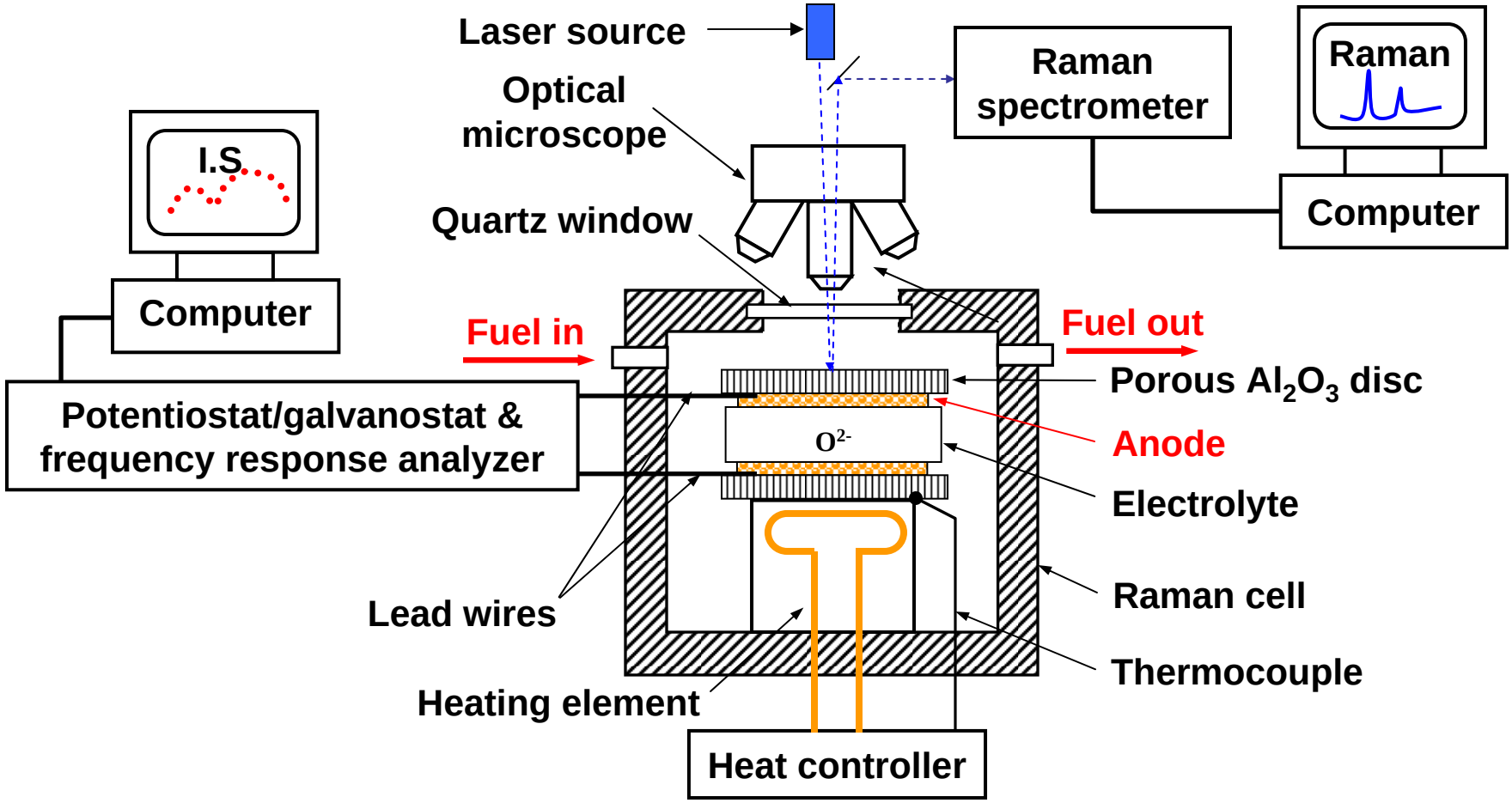

Schematic for the experimental setup of *in-situ* Raman spectroscopy coupled with electrochemical characterization instruments

Raman and DFT results: Ni_3S_2 (Heazlewoodite) Vibrations

Unit cell: #155, R32

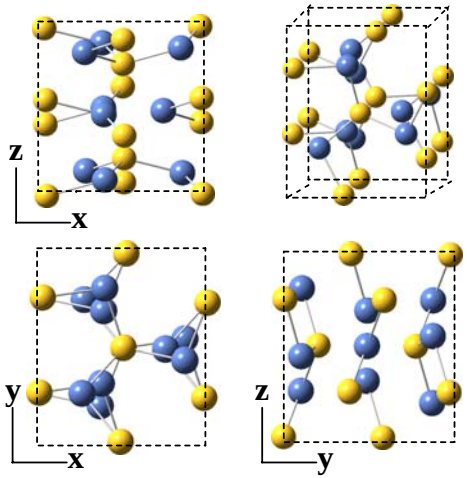

Raman spectrum

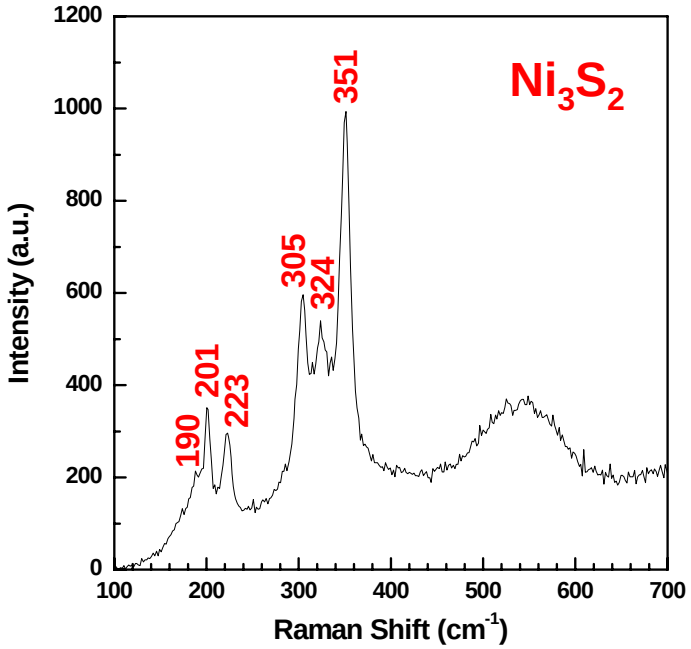

Normal mode analysis:

Total 15 modes:
$2A_1 + 3A_2 + 5E$

6 Raman active:
$2A_1 + 4E$

6 IR active:
$2A_2 + 4E$

2 Translation:
$A_2 + E$

Lattice parameters:

a = 5.751 (5.741)[1]
c = 7.149 (7.139)[1]

Symm.	E		A_1	E		E		E		A_1	A_2		E	
Comp.*	367	367	320	317	316	241	241	204	203	201	0	0	0	
Expt*	361		324	305		223		201		190				

[1] CRC Handbook of Chemistry and Physics. CRC press: New York, 1996

Raman Active Vibration Modes in Ni_3S_2

Vibration modes in a primitive cell

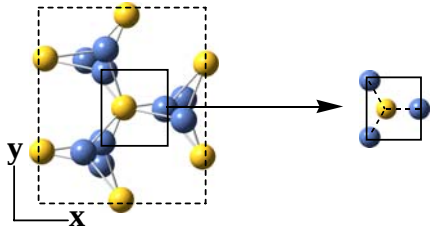

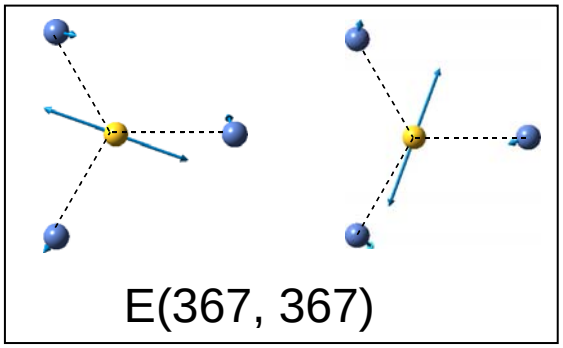
E(367, 367)

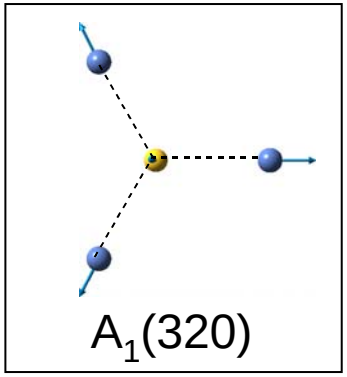
A_1(320)

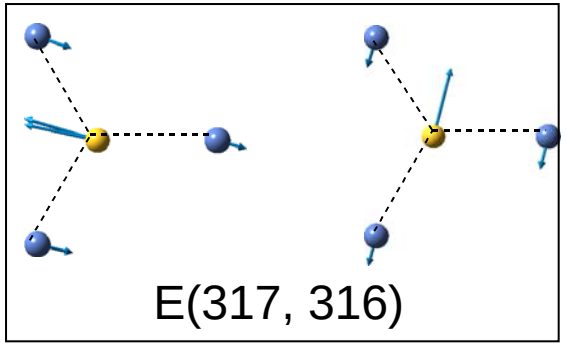
E(317, 316)

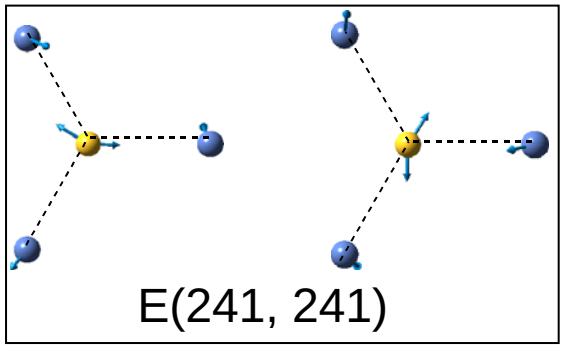
E(241, 241)

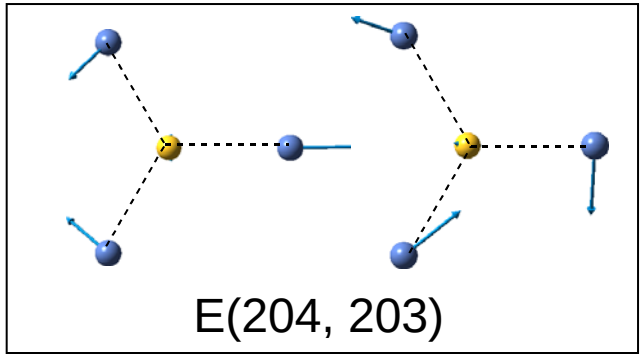
E(204, 203)

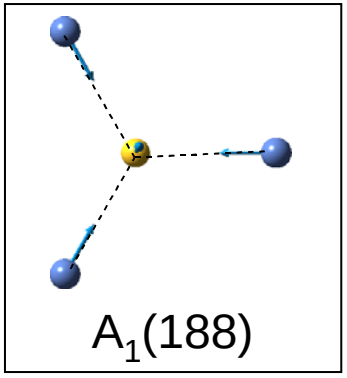
A_1(188)

NiS (Millerite) Vibrations

Unit cell: #160, R3m

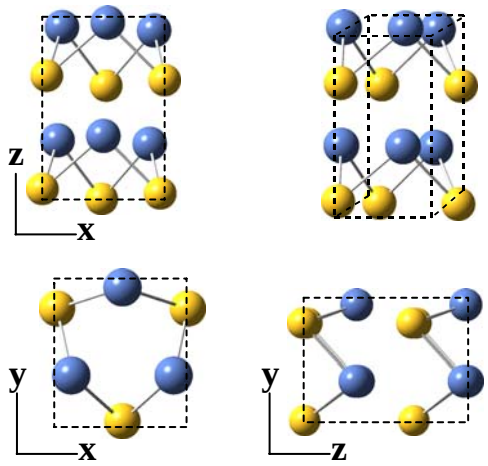

Raman spectrum

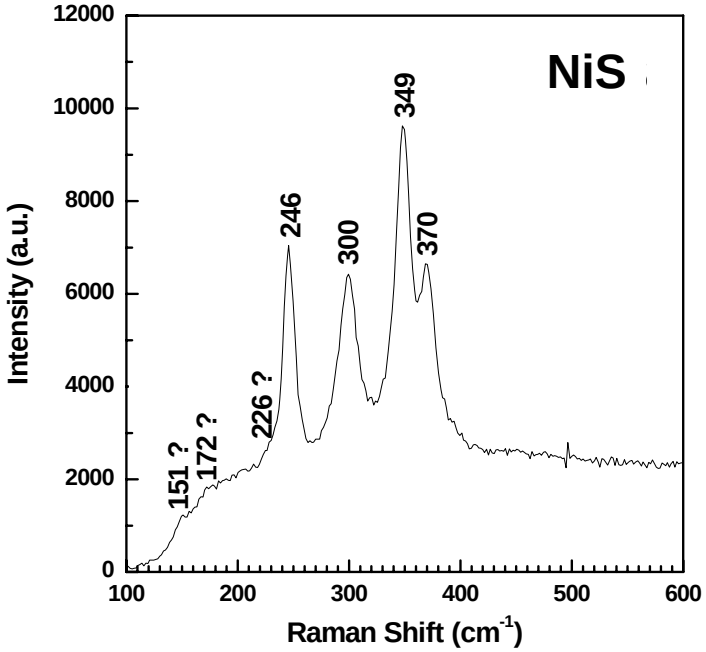

Normal mode analysis

Total 18 modes:
$4A_1 + 2A_2 + 6E$

8 Raman active:
$3A_1 + 5E$

8 IR active:
$3A_1 + 5E$

2 Translation:
$A_1 + E$

Lattice parameters:

a = 9.616 (9.607)[1]
c = 3.154 (3.143)[1]

Symm.	A_1	E		A_1	A_1	E		E		E		E		A_1	E	
Comp*	356	341	341	290	254	252	251	231	230	201	201	148	148	0	0	0
Expt*	370	349		300		246		226		172		151				
Expt[2]	372	350		301	283	246		222		181		142				
Expt[3]	369	349		300	283	244						144				

1 CRC Handbook of Chemistry and Physics. CRC press: New York, 1996
2 Bergo et al., *Mater. Res. Bull.*, 35 (2000).
3 Shen et al., *J. Solid State Chem.*, 175, 221 (2003).

Raman Active Vibration Modes in NiS

In a Primitive Cell

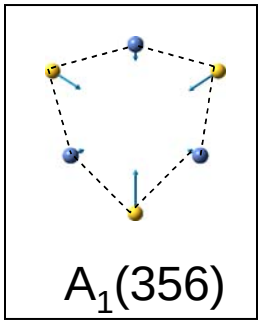

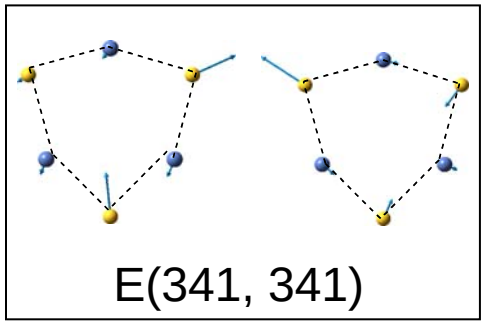

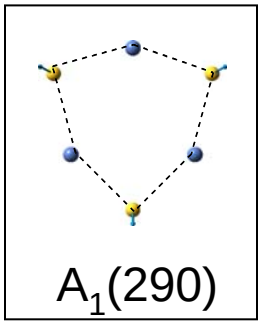

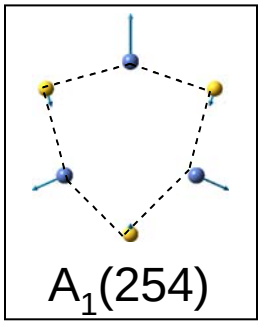

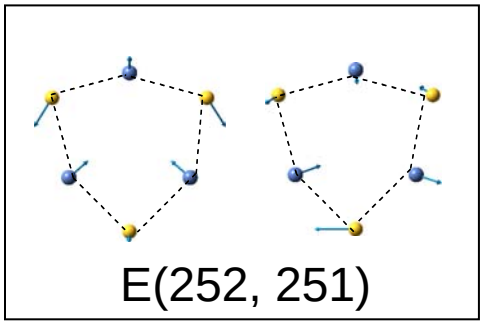

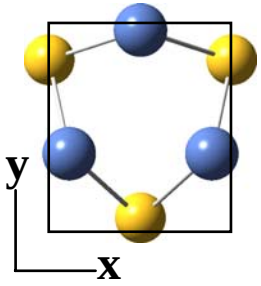

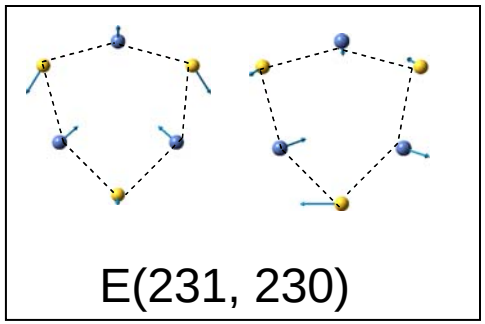

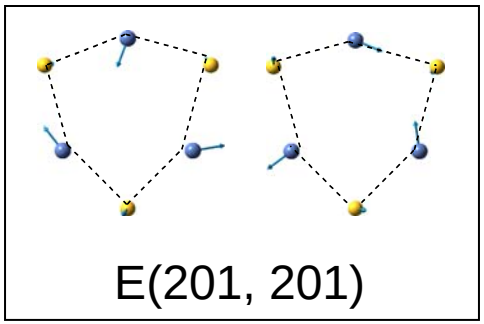

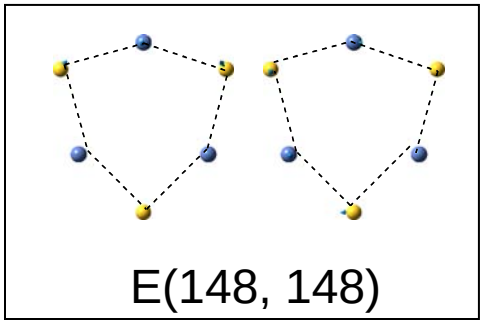

Symm.	A_1	E		A_1	A_1	E		E		E		E		A_1	E	
Comp*	356	341	341	290	254	252	251	231	230	201	201	148	148	0	0	0
Expt*	370	349		300		246		226		172		151				

Ni_3S_4 (polydymite) Vibrations

Unit cell: #227, Fd3m

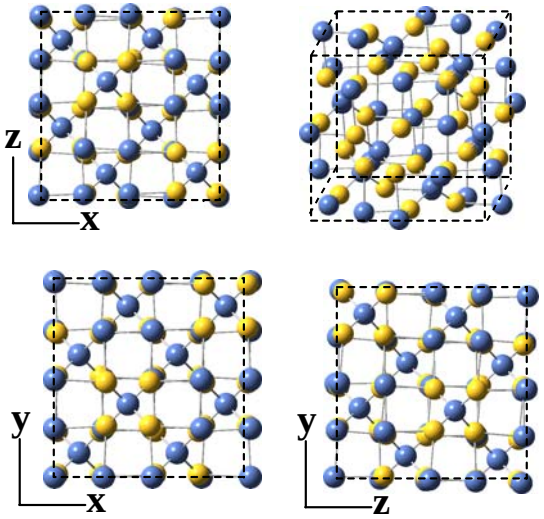

Raman spectrum

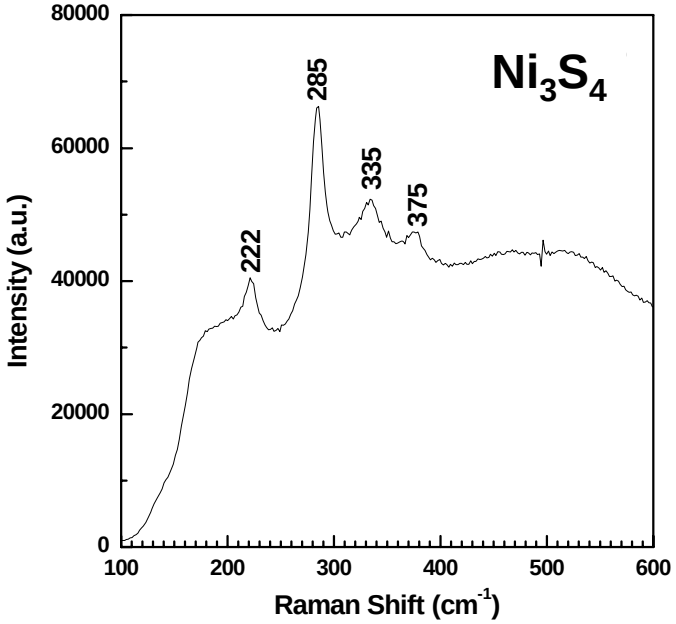

Normal mode analysis

Total 42 modes:

$A_{1g} + E_g + F_{1g} + 3F_{2g}$

$2A_{2u} + 2E_u + 5F_{1u} + 2F_{2u}$

5 Raman active:

$A_{1g} + E_g + 3F_{2g}$

4 IR active:

$4F_{1u}$

1 Translation:

F_{1u}

Lattice parameters:

a = 9.496 (9.405)*

Symm.	A_{1g}	F_{2g}	F_{2g}	E_g	F_{2g}	F_{2u}
Comp*	388 339	338 338 284	284 283	208 207 206	206 205	0 0 0
Expt*	375	335	285	222	208	
Expt[2]	382	337	288	224	208	

[1] CRC Handbook of Chemistry and Physics. CRC press: New York, 1996

[2] Anthony J W, Bideaux R A, Bladh K W, and Nichols M C (1990) Handbook of Mineralogy, Mineral Data Publishing, Tucson Arizona, USA

NiS_2 (Vaesite) Vibrations

Unit cell: #205, Pa3

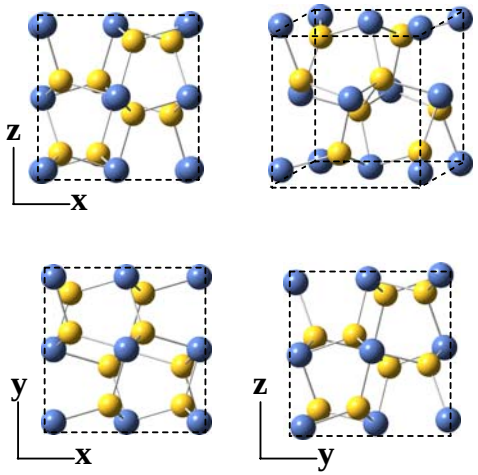

Lattice parameters:

a = 5.620 (5.668)[1]

Raman spectrum

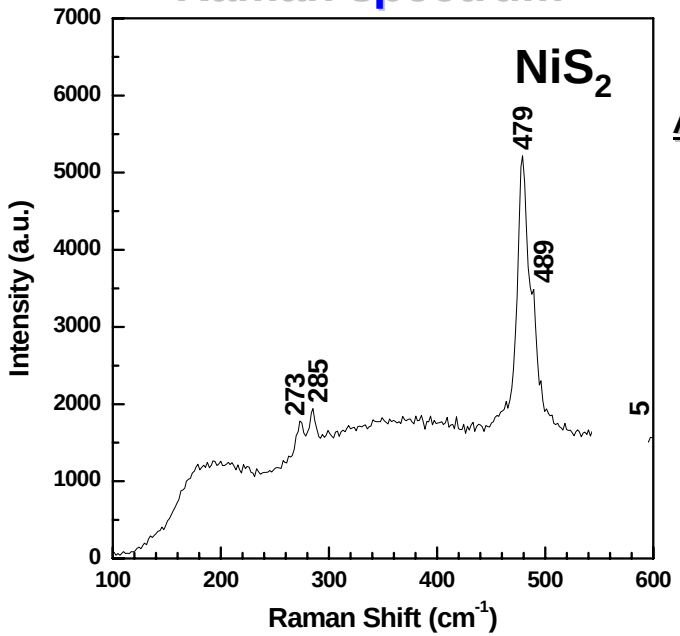

Normal mode analysis

Total 36 modes:

$A_g + E_g + 3F_g + 2A_u + 2E_u + 6F_u$

5 Raman active:

$A_g + E_g + 3F_g$

1 IR active:

F_u

1 Translation:

F_u

Symm.	F_g			A_g		F_g		E_g			F_g			F_{2u}		
Comp*	462	462	461	446	342	341	341	285	285	278	278	277		0	0	0
Expt*		489		479				285			273					
Expt[2]		488		478							281					
Expt[3]		487		480				281			272					
Expt[4]		490		480				285			274					

[1] CRC Handbook of Chemistry and Physics. CRC press: New York, 1996

[2] Anastassakis, Perry, J. Chem. Phys., 64, 3604 (1976).

[3] T. Suzuki, K. Uchinokura, T. Sekine, [illegible]

[4] C. de las Heras, F. Agullo-Rueda, [illegible]

In situ Raman Spectroscopy

Optical images and the corresponding Raman spectra from Ni

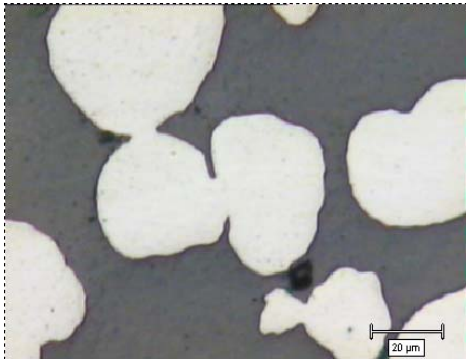

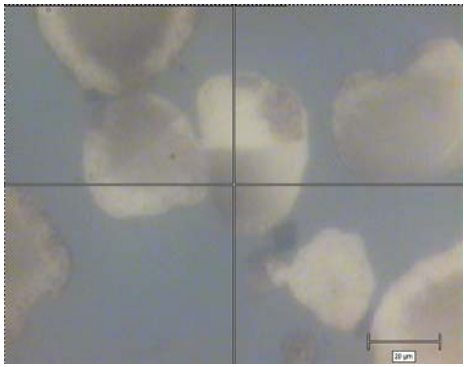

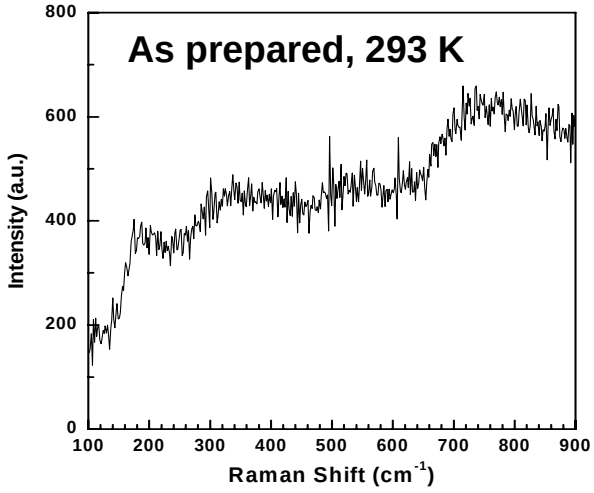

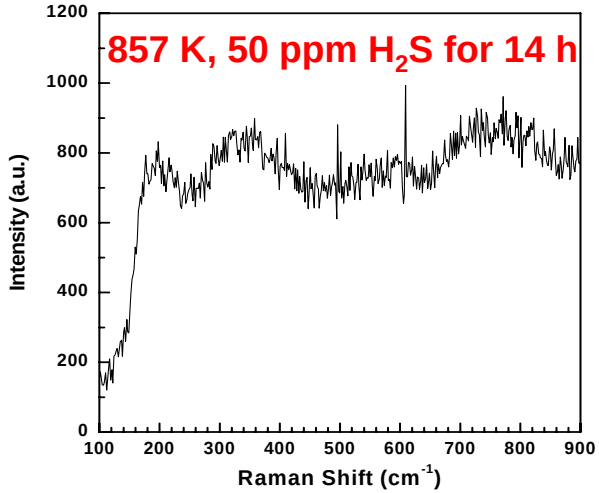

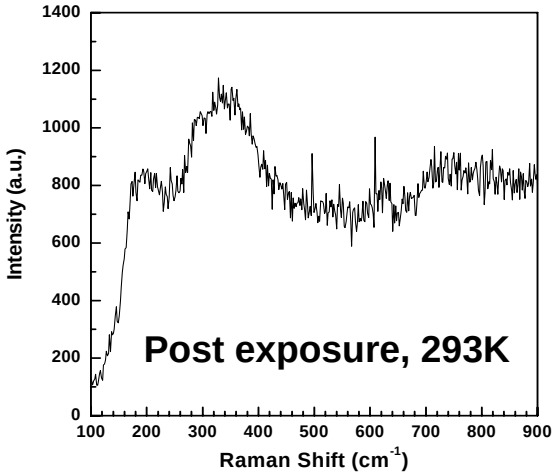

- Formation of nickel sulfides occurs at low temperatures accompanied by dramatic morphological changes

In Situ Observation of NiSx Formation

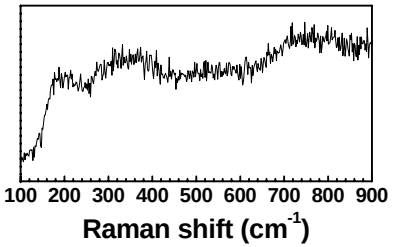

Optical images and the corresponding Raman spectra from Ni region

(15 minutes btw 2 photos)

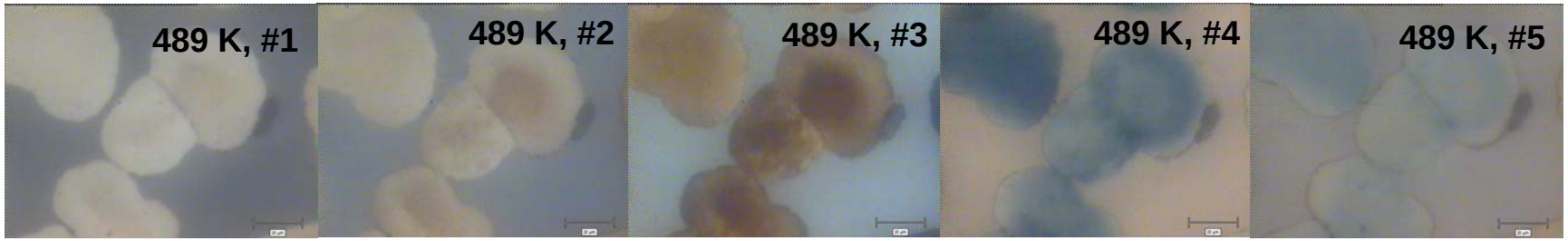

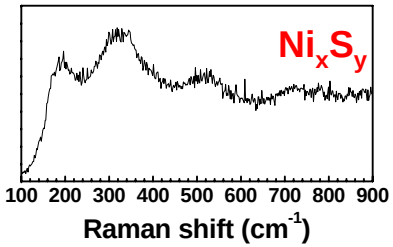

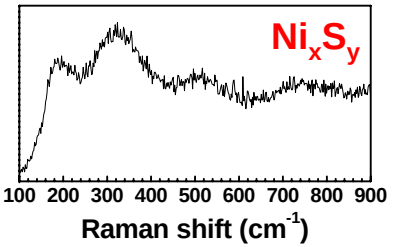

- Nickel sulfides form at lower temperature (<~733K) accompanied by morphology change.

In-situ Observation of Ni_3S_2 at High T

- Ni_3S_2 is Raman active under the the conditions for *in situ* studies at high temperatures (at least up to ~800 K).

293 K

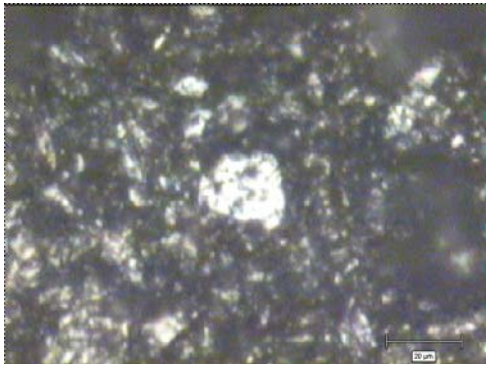

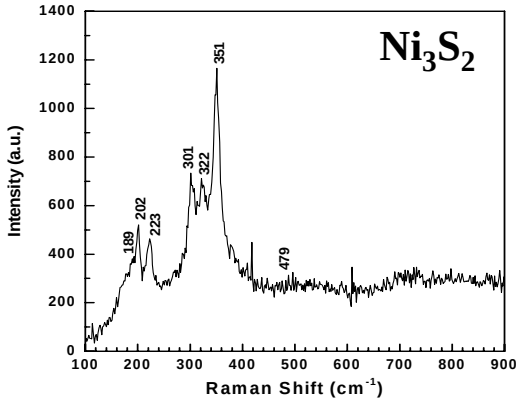

793 K, 50 ppm H_2S/50% H_2/1.5% H_2O/48.5% N_2

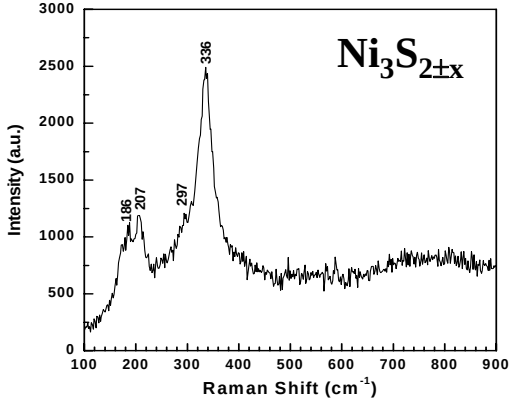

Cooled to 293 K in the same fuel

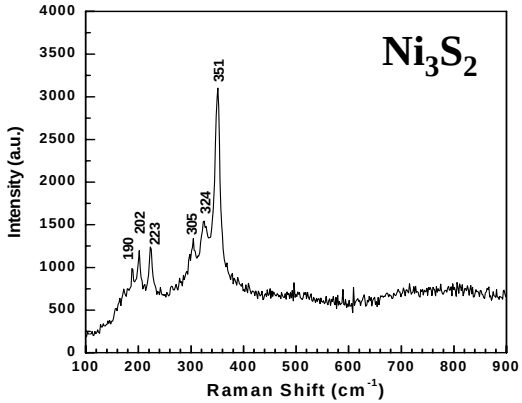

Ni_3S_2 Formation on Ni in **100 ppm H_2S/H_2** at 733K

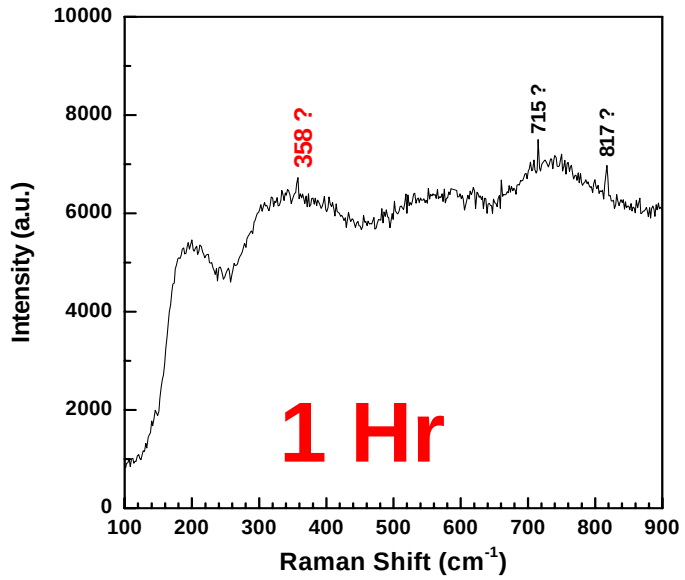

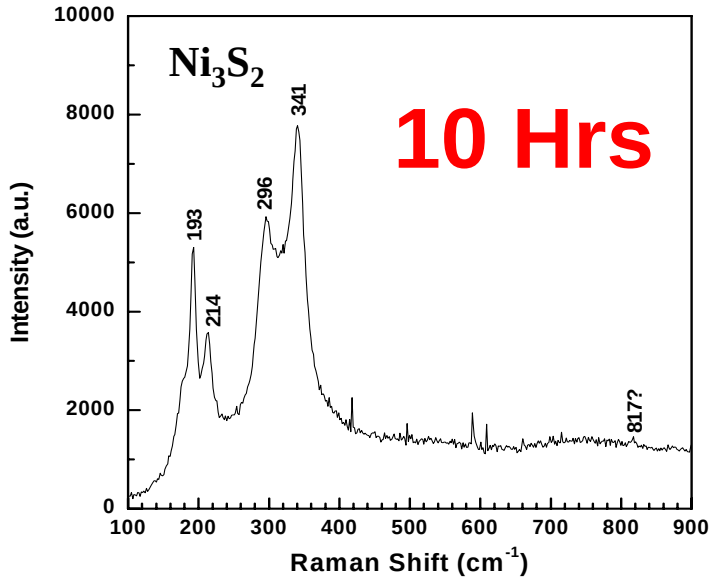

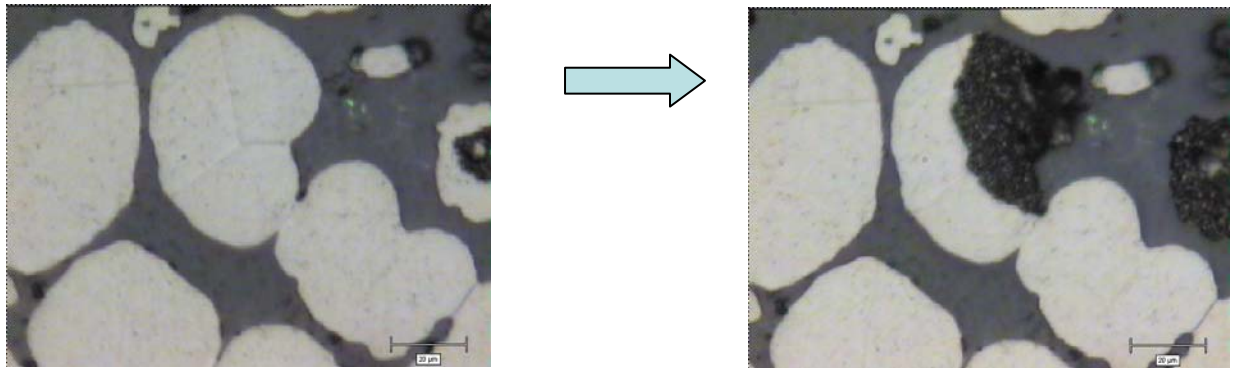

- Formation of Ni_3S_2 was observed under the *in situ conditions*.
- Yet, the sensitivity need to be further enhanced to identify the surface species quickly.

Conclusions – Raman Spectroscopy

- Certain sulfides were detected at high temperatures in sulfur-contaminated fuels; yet, sensitivity needs to be further enhanced.
- Various sulfides form on Ni during cooling accompanied by dramatic changes in morphology, making it difficult to preserve the surfaces for *ex situ* measurements.
- *In-situ* experiment is imperative in the study of sulfur-anode interaction since *ex situ* experiments (SEM, EDX, etc.) could give misleading results due to difficulties in preserving the sample surfaces during cooling.
- Raman is an effective tool for identification of new phases or surface species under conditions relevant to SOFC operation.

How to Achieve S Tolerance?

- Reduce the Adsorption Energy of S on the Electrode (e.g. modification of Ni Surface)

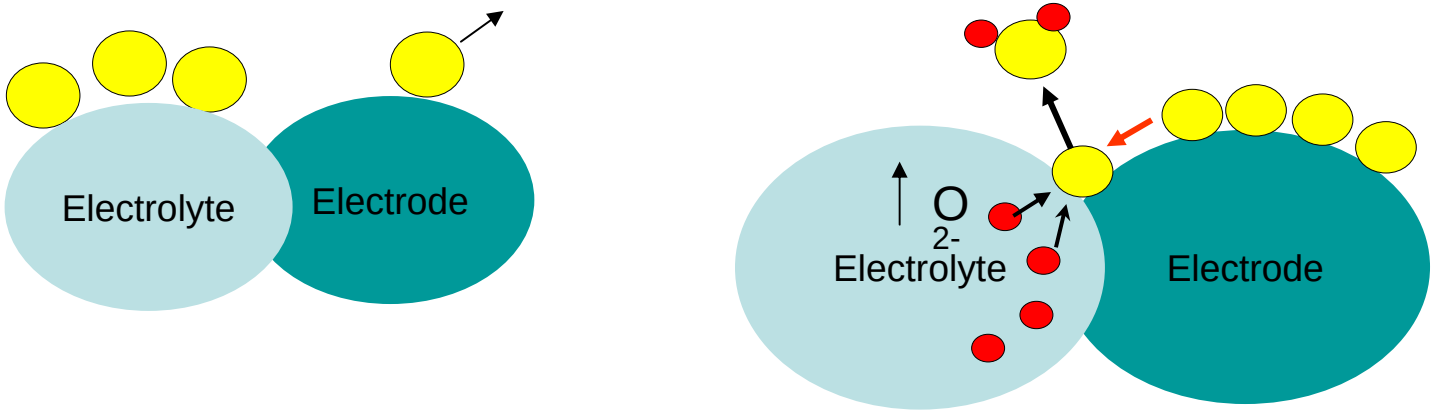

- Remove S from the electrode surface using an electrolyte that promotes electrochemical oxidation of S

Modification of Ni Surfaces

- **Maintain the essential properties of Ni**
- **Modify Ni surfaces with transition metals (*3d* and *4d*)**
- **Determine sulfur tolerance with adsorption-energy calculations btw the surfaces and H_2S**
- **Calculate fuel oxidation (H_2)**

Ni surface modification with 3d & 4d transition metals

Adsorption energy for sulfur tolerance

$\Delta E_{ad} = \Sigma E[products] - \Sigma E[reactants]$

$= E[surface + H_2S] - E[surface] - E[H_2S]$

Ni(111)

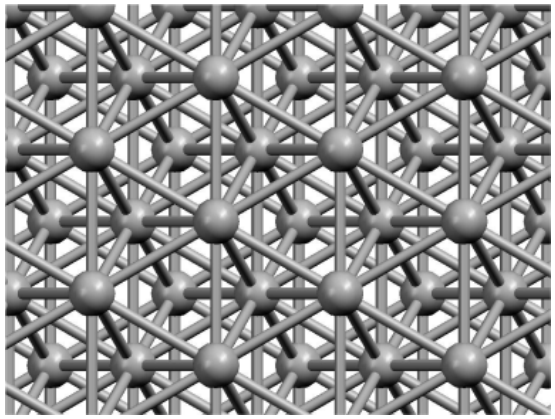

Ni(111) + M

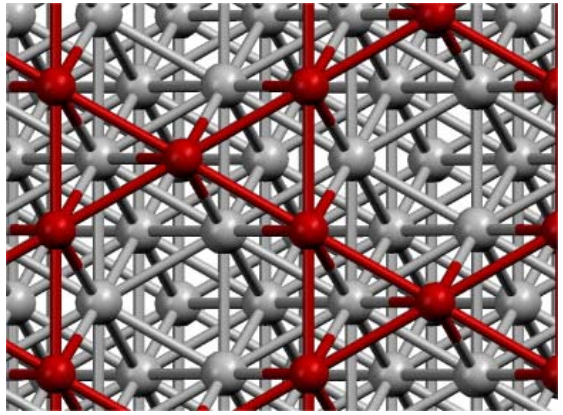

Ni(111)-M + H_2S

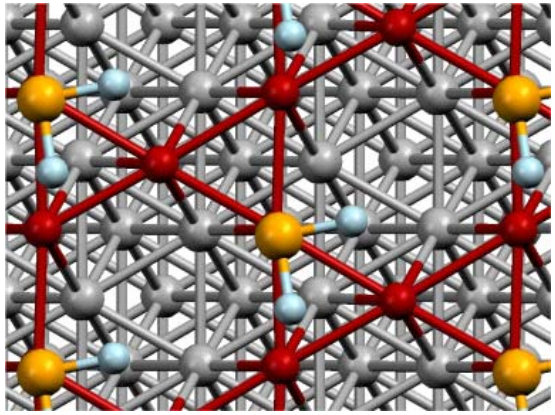

Adsorption energy for dissociative hydrogen

$\Delta E_{ad} = \Sigma E[products] - \Sigma E[reactants]$

$= E[surface + H] - E[surface] - E[H]$

Ni surface modification with 3d & 4d transition metals

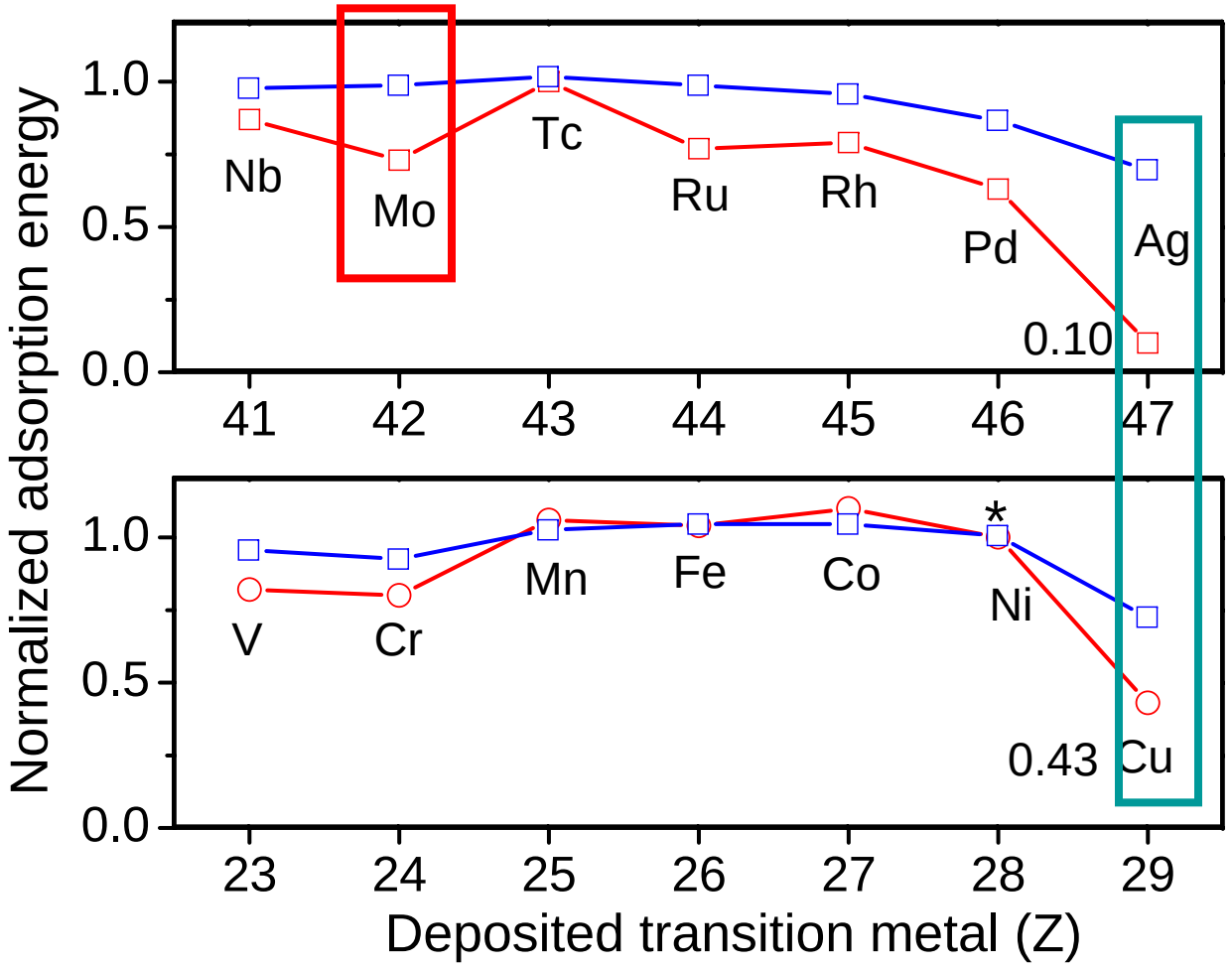

Sulfur tolerance

Dissociative Hydrogen (~fuel oxidation)

5d **W**:
0.86
1.00

Mo and W could be good candidates

Anode: Mo/Ni Impregnated in YSZ

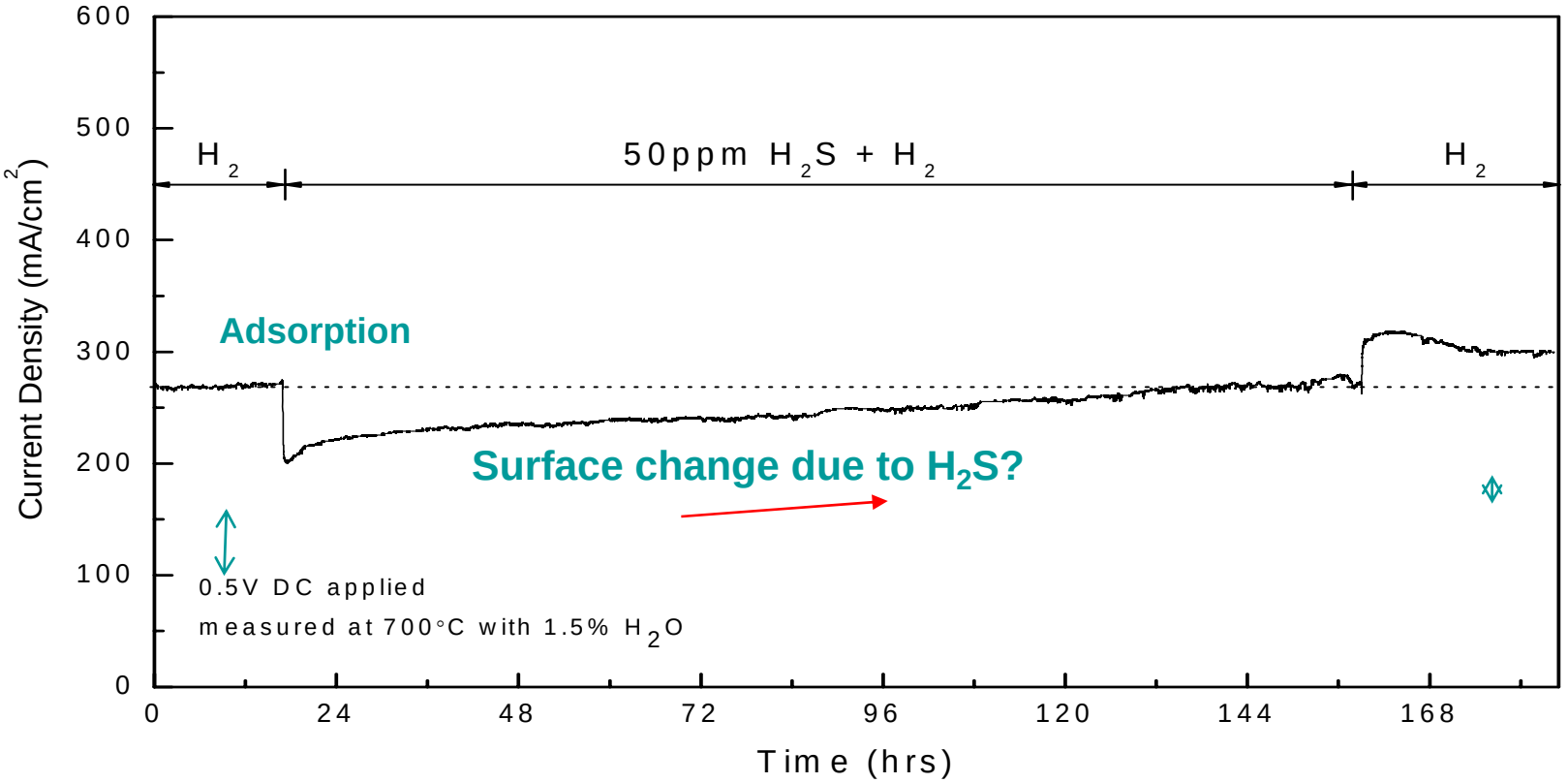

- **No continuous degradation in 50ppm H_2S**
- **The performance gets better during exposure to H_2S**

Materials Modifications

- Mo and W seem to show some promise toward S-tolerance and thus are possible candidates for modifying the surface of Ni/YSZ anode.
- Electrolytes strongly adsorb S may be effective for electrochemical removal of S

Sulfur Adsorption on Electrolyte Surfaces

Modeled surface: the most stable MO_2(111)

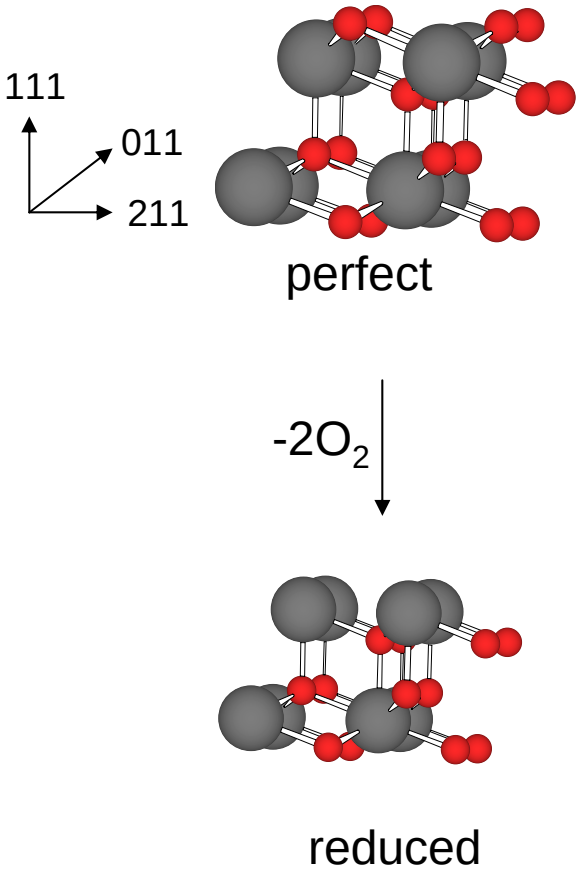

Thermodynamic diagram

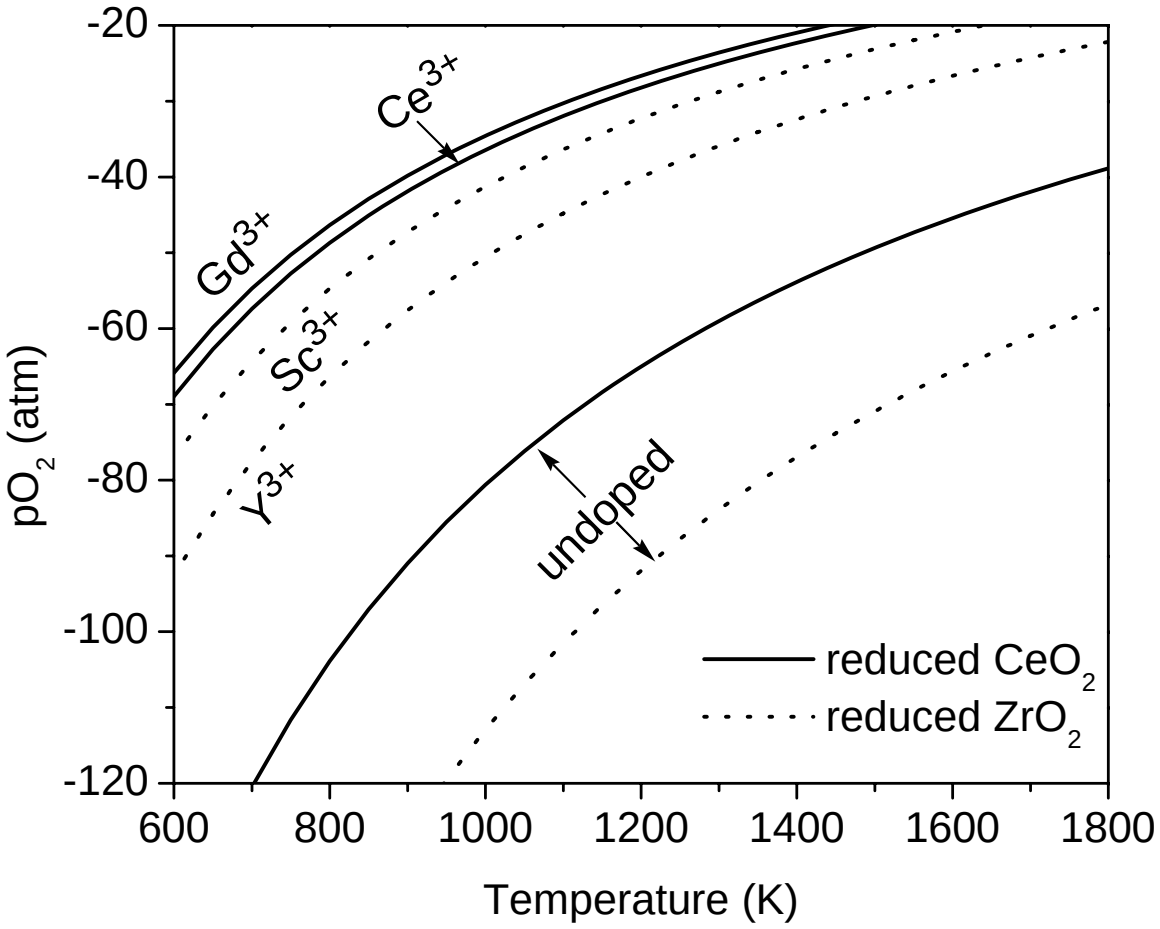

S Adsorption and reduced surface formation energies (eV)

		CeO_2			ZrO_2	
		S(a)	Formation		S(a)	Formation
Perfect	O on top	No ads.		O on top	No ads	
	Ce^{4+} on top	-3.03	8.67	Zr^{4+} on top	-3.67	12.48
Reduced	Ce^{3+}doped	-3.08	4.71	Sc^{3+} doped	-3.36	5.80
	Gd^{3+} doped	-3.06	3.80	Y^{3+} doped	-3.55	7.80

- Sulfur adsorbs strongly on cation-terminated surfaces (< -3 eV), but not on the oxygen-terminated surfaces
- Acceptor-type dopants reduce the formation energy of cation-terminated (reduced) surfaces; the require energy follows the order of

$$Gd_2O_3 < Ce^{3+}{}_2O_3 < Sc_2O_3 < Y_2O_3$$

Summary

- Established a computational framework along with experimental measurements to validate approaches to sulfur tolerance

- CeO_2 + Mo/Ni impregnated anode showed no significant 2nd stage degradation

- CeO_2 addition promoted the electrochemical performance and thermal stability of Mo/Ni impregnated anode

Activities for the Next 6-12 Months

- Further exploration of other strategies for achieving sulfur tolerance and for rational design of new anode materials/structures
- Determination of the practical operation window (T, V/I, H_2S) that minimizes the impact of sulfur contaminants on fuel cell performance, and
- Collaboration with SECA industrial teams to address other issues relevant to sulfur poisoning

Acknowledgement

Lane Wilson, NETL/DoE

SECA Core Technology Program
National Energy Tech Laboratory/ Dept of Energy
DOE Award Number: DE-FC26-04NT42219

PNNL Molecular Science Computing Facilities